Addis Ababa University

Addis Ababa Institute of Technology

School of Mechanical and Industrial Engineering

Numerical Modeling of Mixed Mode Surface Fracture of Carbonized Fe-0.85M0-03C Steel Subjected to Rolling-Sliding Contact

A thesis Submitted to the graduate school in Partial fulfillment of the Requirements for the Degree of Master of Science in Mechanical (Design) Engineering

By: Awet Gebretsadkan

Advisor:

Dr. Samuel Tesfaye

OCTOBER, 2019

ADDIS ABABA, ETHIOPIA

Addis Ababa University

Addis Ababa institute of Technology

School of Mechanical and Industrial Engineering

Numerical Modeling of Mixed Mode Surface Fracture of Carbonized Fe-0.85M0-03C Steel Subjected to Rolling-Sliding Contact

By: Awet Gebretsadkan

Approved by board of examiners

Dr. Samuel Tesfaye	_____	_____
(Advisor)	Signature	Date
Dr. Daniel Tilahun	_____	_____
External examiner	Signature	Date
Behailu Mamo (PhD candidate)	_____	_____
Internal examiner	Signature	Date
Dr. Yilma Tadesse	_____	_____
(Dean of SMiE)	Signature	Date

Declaration

I declare that this work which is being presented in this thesis entitled with "**Numerical Modeling of Mixed Mode Surface Fracture of Carbonized Fe-0.85M0-03C Steel Subjected to Rolling-Sliding Contact**" is the original work of mine where all the work carried out as input according to my knowledge under the supervision of Dr. Samuel tesfaye. The overall work compiles with the regulation of the university and has not been previously submitted for a degree at any higher educational institutions.

Candidate _____ _____

Awet Gebretsadkan Signature Date

This is to certify that the above declaration made by the candidate is correct to the best of my knowledge.

Advisor _____ _____

Dr. Samuel tesfaye Signature Date

Abstract

This thesis is a work in which the surface crack propagation on porous carburized pre alloyed steel subjected under rolling-sliding contact was predicted using numerical approach. The effect of contact load, coefficient of frictional on equivalent stress distribution and pressure distribution is incorporated during FEM analysis In addition, the effect of crack face friction and lubrication pressure, in a mixed mode crack propagation is determined at a mean pressure which shows seeking to generalize the parametric influence on the rolling-sliding contact fatigue. Since the material is porous the initial crack is formed at the center of contact with 2D plain strain condition and elliptical contact parameters determines using Hertz contact theory. The pre alloyed carbonized steel material modelling problem is assumed to be taken as the mean value. Surface propagation is analyzed using energy approach with energy based damage evolution is selected for the crack propagation simulation with extended finite element method. The initial crack propagated at a mean maximum pressure and the coefficient of friction effect is seen, which varies the position of maximum equivalent stress along the surface. When crack face and surface contact friction decrease, the crack length increases and further increase to a large value under the effect of lubrication pressure that results in facilitating crack propagation. The Comparison between the numerical results with the given experimental result shows consistency at a pressure of 960MPa.

Keywords: *Contact stress, Friction, Extended finite Element Method (XFEM), Crack propagation*

Acknowledgements

First of all I would like to express my warmest and greatest as well deepest thankful for my adviser Dr. Samuel, assistant professor in Addis Ababa institute technology for his invaluable input, guidance, and sharing his times, even moral support, throughout this full thesis paper.

I would also like to take this opportunity to grace full for Mr.Behailu (PhD candidate) for supporting and giving clue for having to follow and to know the abacus finite element analysis method working area environment moreover helping in analyzing and identifying the challenges as well to set a recommendation for the best appearance and then just lastly my heartily thankful will shared for my family and miss Ngisti who has provided me through moral and emotional support for her continued support and inspiration during my thesis paper.

Contents

List of tables

List of figures

Nomenclatures

a_o	Crack length	[um]
α_o	Crack inclination angle	[^{o}]
ν	Poisson's ratio	[-]
a	Crack length	[um]
b	Hertzian contact pressure distribution half-width	[mm]
K_I & K_{II}	Mode I and Mode II SIFs	[MPa $m^{0.5}$]
P	Hertzian pressure on the surface	[MPa]
P_c	Fluid pressure inside the crack	[MPa]
P_{max}	Maximum Hertzian contact pressure distribution	[MPa]
μ	Contact surface friction	[-]
μ_f	Friction between crack faces	[-]
P_{crack}	Pressure inside the crack face	[MPa]
E_c	Elastic modulus	[N/$mm^{0.5}$]
R_c	Effective radius	[mm]
K_{Ic}	Fracture toughness rate	[MPa $m^{0.5}$]
G_{Ic}	Fracture energy rate	[N/mm]
σ_y	Yield strength rate	[MPa]
G	Energy release rate	[N/ m^2]
J	J- integral	[-]
H(x)	Heaviside function	[-]
$F_a(x)$	Asymptotic crack tip function	[-]
N_i	Shape function	[-]
u_i	Nodal displacement vector	[-]
F_f	Friction force	[N]
F_N	Normal force	[N]

Abbreviations

SIF	stress intensity factor
RSCF	rolling sliding contact fatigue
LEFM	linear elastic fracture mechanics
EPFM	Elastic plastic fracture mechanics
CZM	Cohesive zone model
FEM	finite element method
XFEM	extended finite element method
RCF	Rolling Contact Fatigue
LCFM	lubricated crack faces mechanism
PM	pressurization mechanism
ETM	entrapment mechanism
MAXPS	Maximum Principal stress Criterion
MAXS	Maximum Principal strain Criterion
MAXE	Maximum nominal stress criterion
QUADS	Maximum nominal strain criterion
QUADE	Quadratic Nominal stress
MAXPE	Quadratic Nominal strain
MTS	Maximum tangential stress
BEM	Boundary Element method
GFM	Greens Function Method
DD	Distributed Dislocations
WFM	Weight Function Method
FEA	Finite element analysis
PN	Phantom node
LSM	Level Set Method
VCCT	Virtual crack closure technique
CTOD	Crack tip opening displacement
CPE4R	Quadrilateral, reduced integration element

Chapter One: Introduction

1.1. Mechanical Contact failure

Fracture or failure of material is a problem that society has been faced for a long period of time as long as there have been many and different man-made structures. Today, the problem is getting worse, because of they used for heavily loaded application which demand to support higher load. Many complex engineering components such as Gears, cams, bearings, gas turbine blades/shafts, railways, bolted flanges and etc. are undergoes rolling-sliding contacts. The contact area (contact zone) is small and higher pressure is developed, that usually result in the fracture of contacting materials. In particular, if the contact load is cyclic, which is obvious for most components, the failure could happen at a lower stress. RSCF is a phenomenon which can lead to a failure of different engineered structures of contacting metallic surfaces. The contact fatigue can be in various ways including yielding, buckling, brittle and ductile fracture [1].

When flaw is presence in the material, stress raise sharply and that result in nucleation of cracks and subsequent grow to a critical length where the structure's strength has been reduced to a point under the application of a cyclic load. Fracture may occur either due to a progressive cracking from the extreme surface or from underneath of the contact interface.

Mechanical components undergo rolling sliding contact subjected to high contact loads at the surface. Different engineering structural components that commonly suffer from cracks at the contact surface due to rolling sliding contact fatigue. RCF is severing disturbance problem at worldwide and results in permanent loss of the component. RCF defects to the United States, Netherlands and European rail system exceeds many millions of dollars annually [2], [3].

Nucleation and growth of contact fatigue crack usually studied using fracture mechanics approach with the help of numerical models. Various numerical methods such as the finite element method, the boundary element method and the finite difference method have been developed and applied in fracture mechanics. Among all numerical methods, the FEM and XFEM is the most widely used as a tool for the solution of practical engineering fracture problems due to its ability to deal with the awkward geometries and complicated boundary conditions in a unified manner. For modeling crack propagation, a general 2-D crack propagation model is developed using both conventional FEM and XFEM approaches. The Finite Element Method has been used for the past few decades to assist engineers in analyzing the most complex, cracked structures. Until recently, cracks had to

be modeled as part of the structure's geometry. As the crack grew, the model would be rebuilt and re-meshed, requiring significant user interaction or specialized programs [1].

Many previous laboratory studies of the rolling-sliding contact fatigue behavior of steels have been performed on twin-disc wear machines. The relationship between rolling-sliding contact fatigue, contact stress, creep, microstructure and surface events for a range of pearlitic rail steels were examined in [4]**.** Figure 1.1 represents the damaged surface of pinion due to contact fatigue test.

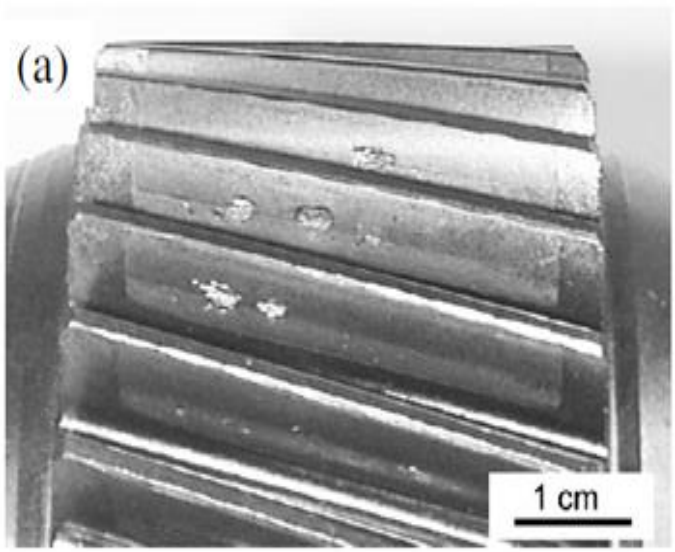

Figure 1. 1 Surface initiate damage of the pinion that was subjected to rolling-sliding contact [5]

The repeated load cycle on the contact zone could promote initiation and growth of cracks. First, crack were nucleated at the surface that is mainly due to shear stress, then the subsequent propagation to a certain depth from the surface (due to tensile and shear stress) and branching of cracks results in surface particle detachment; as that are observed at the surface of the pinion. This type of surface damage results in permanent loss of the pinion; that contributes the hug effect on the global economy. Therefore, the investigation of surface damage due to contact load is a very active research area.

Many researches were carried out to analyze surface initiated cracks either using theoretical or experimental approaches. In paper [6], the surface damage of pre alloyed steel subjected under rolling sliding contact was investigated. In the paper, initially the theoretical resistance to nucleation of surface cracks were predicted using stress failure criterion approach, then experiment (disk on disk contact fatigue) were carried out to validate the theoretical resistance. The material

was sintered steel that have porosity on its microstructure. Figure 1.2 represents the worn microstructure of porous sintered steel (Fe-0.85Mo-0.35C steel) tested at 950MPa mean hertzian pressure.

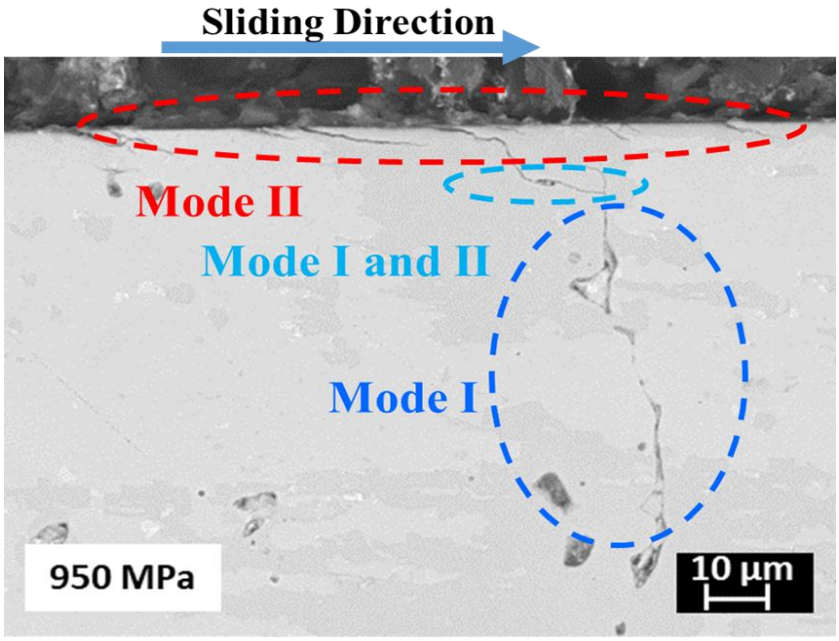

Figure 1. 2 Worn microstructure tested at 950 MPa mean Hertzian pressure

First micro crack was nucleated at the surface, which is due to mode II (shear mode) loading of the crack, then the crack start to grow towards the bulk in mixed mode condition. The transition of crack propagation from mode II to mode I and II loading condition relates with the application of additional stress due to lubricant pressure and friction force at the crack faces. As crack size grow deeper, lubricant pressure and crack face friction stress become higher at the crack tip that results in crack propagation in opening mode of fracture (Mode I).

In this work, which is the continuation work from paper [6], surface cracks propagation is analyzed using numerical approach. First the initial nucleation crack is observed from the experiment taken simply as initial crack by comparing the contact equivalent stress determined from numerical analysis and the strength of the material. Then crack propagation and the effect of lubricant pressure and crack face friction were studied simply by simulating a numerical model using abacus software. In addition, the effect of applied load and friction (at the contact surface) on the distribution of equivalent stress and contact pressure were analyzed.

1.2. Problem statement

Surfaces that are repeatedly loaded by rolling-sliding contact usually be exposed to fail by contact fatigue. Nowadays almost all the motion produced are in mechanical contact for transferring power, torque and speed in typical mechanical applications , such as gears, cams, bearings and rail/wheel. Many surface and subsurface failure estimated to comprise approximately 90% of all metallic fatigue damage failures has been recorded due to mechanical cause because of used for heavily loaded application which demand to support higher load and light in weight with design problem, lack of regular scheduling maintenance.

Currently the material are carburized by adding some percent of carbon content to the outermost shell of the material which expose to contact for hardening to resist high load which leads severe in failure such as crack initiation, propagation and pitting.

The combination of compressive load and mechanical fatigue on the rolling sliding contact materials affects the propagation of crack. Different researches seek study on crack initiation and propagation due to different condition using the conventional FEM approach but this thesis concern on study crack propagation of Carbonized Fe-0.85M0-03C Steel with an initial crack at the surface by using surface based cohesive zone model formulation approach under XFEM. So that this is highly demanded to study the crack propagation accurately under the selected parameter and so numerical methods have to be used to predict and analyze failure on materials.

1.3. Objective

1.3.1. General objective

The main and general objective of this thesis is to investigate a mixed mode surface fracture of porous Carbonized Fe-0.85M0-03C Steel subjected under rolling-sliding contact using the numerical modeling.

1.3.2. Specific objective

- Investigation of parametric effects, such as friction and applied load on Von Mises and contact pressure distributions.
- Modeling of mixed mode surface fracture using XFEM (abaqus) simulation software's.
- Determining stress intensity factor at the crack tip and predicting crack propagation based on the toughness of the material.
- Comparing numerical model results with the experimental results (validation)

1.4. Scope and Delimitation of the study

This study deals with the mixed mode (I and II) surface fracture of material subjected under rolling sliding contacting using finite element method. The stress intensity factor at the crack tip will be determined, and the variation of influential parameters such as contacting load, friction and lubrication will be investigated. Lastly, this study will compare the numerical results with analytical and experimental results made by paper [6]. But this work will not consider other parameters such as the effect of surface roughness, fluid film thickness, temperature, material type, geometry and residual stress. The crack propagation analysis is only based on CZM approach; and the analysis will be limited to homogeneous in property and isotropic materials.

Chapter Two: Literature Review

2.1. Contact mechanics

Contact mechanics considers the analysis of material responses when the bodies are in contact. This interaction or contact can occur on many different scales, ranging from Nanoscale asperities up to tires on roads and even contact between tectonic plates. Contacts can and do cause very high stresses between objects that can cause failure or fracture in the form of contact fatigue, yielding, surface fatigue, and wear [7].

Contact mechanics is concerned with stresses and deformations that arise when the surfaces of two solid bodies are brought into contact. The contact can be either conforming or non-conforming. Conforming contact is the contact where the surfaces of the two bodies fit each other exactly or very closely without deformation. In the contrast, the contact of bodies with dissimilar profiles is characterized as non-conforming. The contact area of the non-conforming contact is generally small comparing with the dimensions of the bodies themselves. The stresses are highly concentrated in the region close to the contact zone and are not greatly influenced by the shape of bodies at a distance from the contact area. Common engineering applications of non-conforming contacts are wheels, bearings, traction drives, gears and cams [8].

2.1.1. Hertzman contact

The benchmark work of Hertz (1882) considered the contact between normally loaded non-conforming bodies, which are homogenous in microstructure (material), frictionless surface and undergoes only elastic deformation, to analyze surface deformation shape and contact stress distributions [9]. The Hertzian formulation of contact between cylinders, which can be equated to a cylinder-on-half-space equivalent, is used to calculate the stress state of a pure material at a specific depth and location. Moreover, Hertz provides a paper for his study to form a closed-form solution to the normal contact problem having made the following assumptions:

- The contact is elastic
- The material of the disc is applied in the elastic area
- A quasi-static analysis is considered. Because of very low deformation and strain of the slave disc
- The width of the contact is small compared to the body radii
- Profile is smooth, continuous and non-conforming.

Figure 2. 1 Illustrates ring on ring hertzian contact and the hertzian pressure distribution within the contact width (2b).

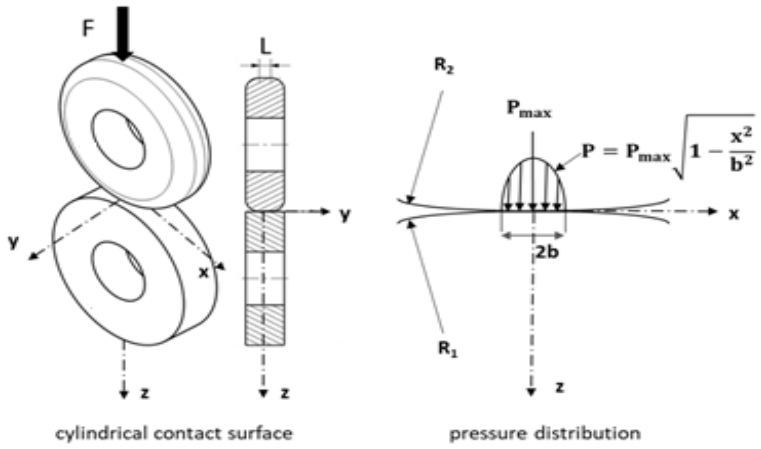

Figure 2. 1 Contact between cylindrical surfaces and parabolic pressure distribution [10]

According to the Hertzian contact theory, the pressure distribution (P) is parabolic in shape in the contact width (2b); pressure becomes maximum (P_{max}) at the middle of the contact zone.

The 2-D Hertzian stress distribution on x-z plane determines using formulas eq. (2.1) to eq. 2.5).

$$\sigma_x = \frac{P_{max}}{b}\left\{m\left(1+\frac{z^2+n^2}{m^2+n^2}\right)-2z\right\} \tag{2.1}$$

$$\sigma_z = \frac{P_{max}}{b} m\left(1-\frac{z^2+n^2}{m^2+n^2}\right) \tag{2.2}$$

$$\sigma_y = \nu(\sigma_x+\sigma_z) \tag{2.3}$$

$$\tau_{max} = \begin{cases} \tau_{xz} = \dfrac{\sigma_z-\sigma_x}{2}, & \dfrac{z}{b} < 0.463 \\ \tau_{yz} = \dfrac{\sigma_z-\sigma_y}{2}, & \dfrac{z}{b} > 0.463 \end{cases} \tag{2.4}$$

$$\sigma_{eq.} = \frac{1}{2}\left[(\sigma_z-\sigma_x)^2+(\sigma_y-\sigma_x)^2+(\sigma_z-\sigma_y)^2\right]^{0.5} \tag{2.5}$$

Where, m and n are variables described in terms of space X, Z coordinate and determined eq. (2.6) and (2.7), respectively.

$$m^2 = \frac{1}{2}\left[\ \{(b^2-x^2+z^2)^2+4x^2z^2\}^{\frac{1}{2}}+(b^2-x^2+z^2)\ \right] \tag{2.6}$$

$$n^2 = \frac{1}{2}\left[\ \{(b^2-x^2+z^2)^2+4x^2z^2\}^{\frac{1}{2}}-(b^2-x^2+z^2)\ \right] \tag{2.7}$$

The sign of m and n are associated with the sign of z and x axis, respectively.

The mean Hertzian pressure (P_o) applied on the cylindrical contact surface is determined using the relation given by eq. (2.8).

$$P_0 = 0.78P_{max} \tag{2.8}$$

Where maximum pressure is given by eq. (2.9)

$$P_{max} = \frac{2F}{\pi bL} \tag{2.9}$$

Half contact width b relates to the effective elastic modulus (E_c), the effective radius (R_c) of curvature, and the applied load (F) and is determined using eq. (2.10).

$$b = \sqrt{\frac{4R_cF}{\pi LE_c}} \tag{2.10}$$

Where E_c and R_c are evaluated using eq. (2.11) and eq. (2.12), respectively.

$$\frac{1}{E_c} = \frac{1-{\nu_1}^2}{E_1} + \frac{1-{\nu_2}^2}{E_2} \tag{2.11}$$

$$\frac{1}{R_c} = \frac{1}{R_1} + \frac{1}{R_2} \tag{2.12}$$

2.1.2. Rolling-sliding contact

When two rotating mechanical elements brought into contact with each other, pure rolling, rolling-sliding, or sliding contacts may depend on the relative velocity of the contacting bodies. In the case of gear teeth contacts, the pure rolling contact occurs at the pitch points of the involute profiles of the teeth because no relative velocity at the pitch point. However, slip or sliding occurs due to relative velocity at the other contact situations along the path of contacts. Therefore, the gear teeth rolling contacts are in essence rolling-sliding contacts. In addition, bearings and other mechanical components undergo rolling sliding contacts. These type of contacts are mostly experimentally studied using a two-disc wear machine to characterize contact fatigue behavior [11].

The rolling contact fatigue of the disc contact is often categorized based on the distance of where the cracks are initiated compared to the surface of the wheel these are:

- Surface initiated fatigue
- Subsurface initiated fatigue (0.1 to 0.4 mm from the surface)

The subsurface cracks are rare, yet this crack is the most dangerous one when it is compared with the surface cracks. Where there exist a low fatigue resistance of the material such as microscopic manganese sulphide inclusions or even voids, there are great risks for both of the phenomena to

occur. Surface initiated cracks are conversely gives warning time and with through re-profiling (example rail-wheel interaction) of profiles or even by regular natural wear.

2.1.3. Equivalent Hertzman contact model

For computational simulations of non-conforming contact of mechanical elements it is advantageous to use a substitute model of two contacting cylinders instead of simulating the actual contact [8]. In the case of a two-disc machine, where the upper disc has a crown radius and the bottom disc is cylindrical, the apparent contact area is elliptical. At the outermost circumference, the two discs rotate with velocities V_1 and V_2, where $V_1 \neq V_2$. The existence of slip between the discs together with normal load acting on them, results in sliding wear. Such a system is similar to the one shown on the right-hand side in which the bottom disc is fixed and the top disc rotates at the slip velocity $V = |V1 - V2|$. With this assumption, the problem can be reduced from a rolling-sliding contact to a quasi-static sliding contact [9], [11].

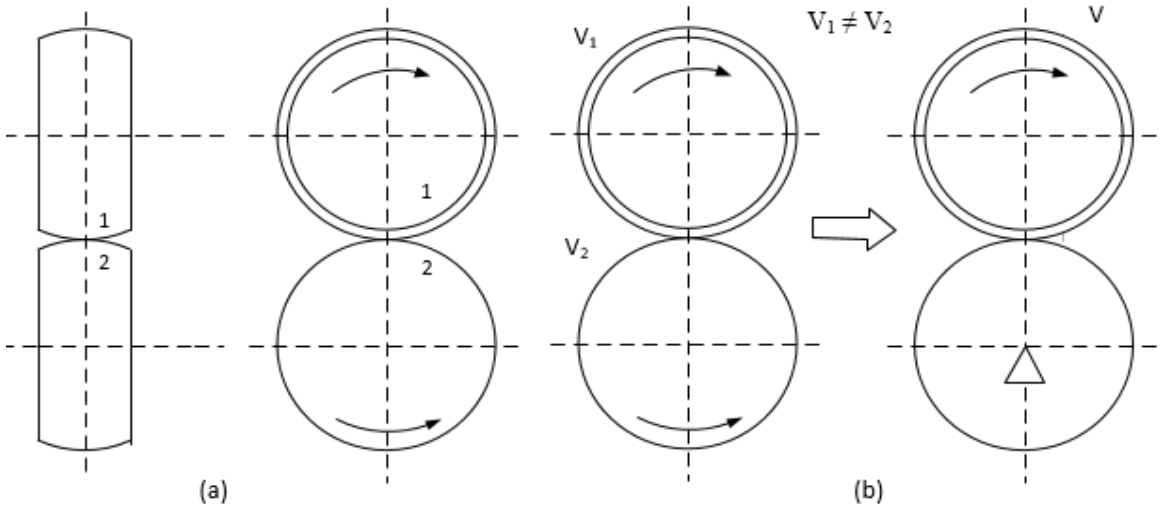

Figure 2. 2 (a) Schematic of the two-disc machine, and (b) model simplification of rolling-sliding contact with defined slip to sliding contact in two disc tribometer [9], [11]

Through the action of a force, F, cylindrical surfaces with the radius R_1 and R_2, brought into physical contact and initially forms a line contact. The parabolic pressure distribution is build-up at the contact zone over the contact length, and the pressure is the maximum at the center of the contact width this configuration of contact represents the real machine element contacts, such as cam and gear teeth interaction with the counter face. Often the contact area is small, and higher contact stress is applied to the contact zone, that results in elastic or elastic-plastic deformation in the surface layers.

2.2. Tribology

Tribology is the science and technology of friction, wear and lubrication that studies the interaction of surfaces in relative motion. It concerns the understanding of a wide range of applications, from simple everyday products to complex industrial machinery [9].

Friction is the force resisting the relative motion of solid surfaces, fluid layers, of material elements sliding against each other they can be Dry Friction and Fluid Friction.

Wear is a continuous loss due to surface material to rubbing action related to interactions between surfaces and specifically the removal and deformation of material on a surface as a result of mechanical action of the opposite surface. Wear are different types which are Adhesion Wear, Abrasive Wear, Surface fatigue, Fretting Wear and Erosive Wear and Lubricants are agents introduced between two surfaces in relative motion to minimize friction [12].

The interactions of mechanical loading and chemical/electrochemical reactions that occur between the elements of a tribological system exposed to biological environments constitute bio-tribo corrosion science [13]. The surface is normally defined as the boundary between the environment and the material. The study of surfaces in relative motion, in contact and under pressure that of tribology.

Flat rolling of metals, focus on three interconnected phenomena: friction, lubrication and wear at the contact surfaces. In the metal rolling industry the costs associated with wear problems account for nearly 10% of total production costs [14].

2.3. Fracture mechanics

Fracture mechanics is the field of solid mechanics that deals with the behavior of cracked bodies subjected to stresses and strains. These can arise from primary applied loads or secondary self-equilibrating stress fields such as residual stresses and stress concentration. This high localized stress leads to failure of components that result in material loss, casualties and injuries [15].

Fracture mechanics is to characterize the local stress distribution and deformation around a crack tip in terms of the asymptotic field around the crack tip scaled by parameters that are a function of the loading mode, crack position and global geometry.

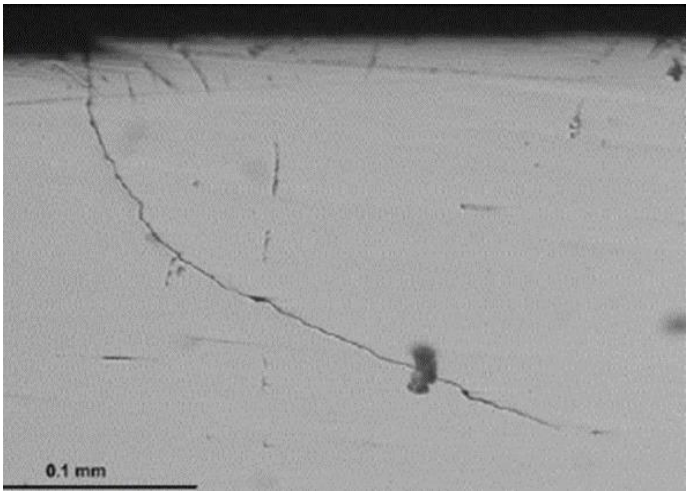

Figure 2. 3 Surface contact failure section of a ring/cone crack at an angle to the surface [16]

2.3.1. Type of fracture

Engineering materials, such as metals, have two primary modes of fracture: brittle and ductile.

Brittle fracture: Cracks spread very rapidly with little or no plastic deformation and Cracks that initiate in a brittle material tend to continue to grow and increase in size provided the loading will cause crack growth.

Ductile fracture: usually ductile material has three stages: void nucleation, growth, and coalescence. The crack moves slowly and is accompanied by a large amount of plastic deformation. The crack typically will not grow unless the applied load is increased. Different theories have been advanced to describe the fracture process in order to develop a predictive capability that is LEFM, Cohesive zone models and EPFM.

2.3.2. Linear Elastic Fracture Mechanics

Linear Elastic Fracture Mechanics have been first introduced by Griffith, the idea was to explain the behavior of flaws in specimens. The first relation proposed is between applied stress $\boldsymbol{\sigma}_{app}$ and the square root of the crack length. This relation is constant. Griffith first tried to explain the connection using the classic linear elastic theory. This technique brought some problems, since the stress at the tip of a sharp flaw becomes infinite. The theory was therefore explained using energy considerations, which have been better refined by Irwin [16].

The objective of LEFM is to predict the critical loads that will cause a crack to grow in a brittle material. LEFM always requires a pre-existing flaw. The concepts of LEFM, such as the stress intensity factor and the strain energy release rate are based on describing the stress or energy state in the vicinity of a crack tip. If there is no crack tip these concepts make no sense. Thus LEFM

cannot predict initiation from 0 crack length. However you could assume the presence of a very small flaw and assume that a crack will initiate under the same conditions that would cause that flaw to propagate. The local stresses in the vicinity of a crack tip are analyzed according to the theory of elasticity in linear elastic fracture mechanics.

Linear Elastic Fracture Mechanics considers three distinct fracture modes: Modes I, II, and III. These encompass all possible ways a crack tip can deform.

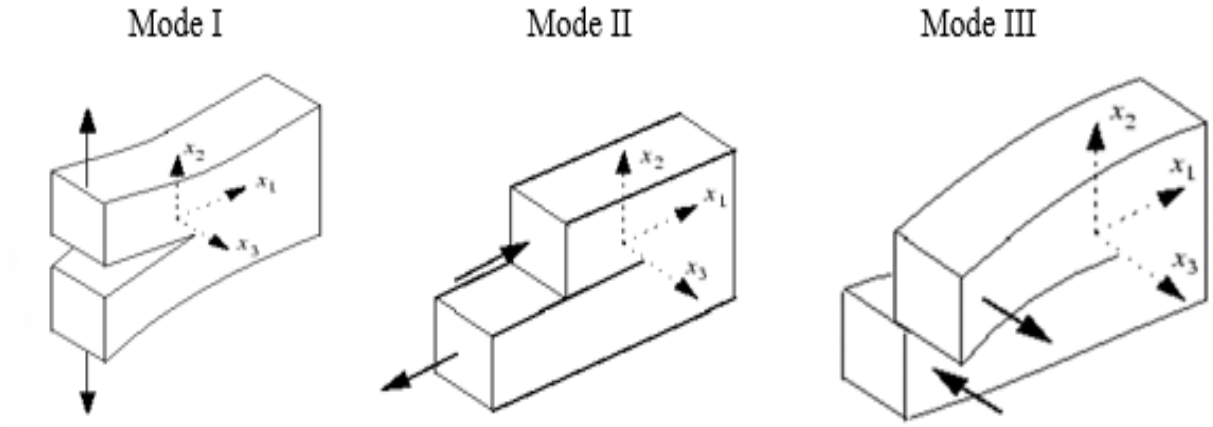

Figure 2. 4 Three modes of displacement at crack tip

The most Four well accepted parameter to measure the potency of a crack are Energy release rate (G), Stress intensity factor (K), J- integral (J) and Crack tip opening displacement (CTOD)

Energy release rate is energy based and is applied for brittle or less ductile materials. Stress intensity factor is stressed based, also developed for brittle or less ductile materials. J- Integral has been developed to deal with ductile material. It formulation is quite general and can be applied to brittle materials also. Crack tip opening displacement is displacement based which was developed for ductile materials [17].The Influence contact load, crack shape, depth and friction coefficient between crack's surfaces is presented and finite elements method is used for simulation of rolling of cracked ball by applying the LEFM, the crack determines in terms of stress intensity factors. The reduction of the crack angle yields the decrease of K_{II} and increases K_I [18].

2.3.3. Stress Intensity factor

Is one of the most fundamental parameters in all of fracture mechanics which describes the stress state at a crack tip, related to the rate of crack growth, and is used to establish failure criteria due to fracture. The stress intensity factor was developed in 1957 by George R Irwin, arrived at the definition of K near-crack-tip approximation and Westergaard's complete solution for the stress field surrounding a crack.

The stress intensity factor defines the amplitude of the crack-tip singularity and it predicts stress intensity near the tip of a crack caused by a remote load or residual stresses.

For isotropic, linear elastic materials, LEFM characterizes the local crack-tip stress field in the linear elastic (i.e., brittle) material using a single parameter called the stress intensity factor *K*.

The magnitude of K depends on:

- Sample geometry
- Size and location of the crack
- Magnitude of load
- Distribution of load

The stress intensity factor is a single-parameter characterization of the crack tip stress field. The following equation describes stress intensity:

$$\sigma_{ij}^{Tip} = \sigma_{ij}^{Tip}(location, loading, geometry) \tag{2.13}$$

$$\sigma_{ij}^{Tip} = \sigma_{ij}^{Tip}(r, \theta, K) \tag{2.14}$$

Where location can be represented by r and using the polar coordinate system whereas the loading and geometry terms can be grouped into a single parameter *K*, called the stress intensity factor

For a through crack in an infinite plate under uniform tension, the stress intensity factor is

$$K = \sigma\gamma\sqrt{\pi a} \tag{2.15}$$

Where γ describes the relationship between gross geometrical features to the stress intensity factors. γ Can be a function of crack length as well as other geometrical features. σ Represents nominal stress that is remote from the crack.

The above equation shows that the intensity of the stress field and therefore the stresses in the crack tip region are linearly proportional to remotely applied stress and proportional to the square root of half the crack's length. Stress intensity can be determined by Finite element analysis, ASTM standard method and Weight function method. Crack tips produce $\frac{1}{\sqrt{r}}$ singularity and the stress fields near a crack tip of an isotropic linear elastic material can be expressed as a product of $\frac{1}{\sqrt{r}}$ and a function of θ with a scaling factor K.

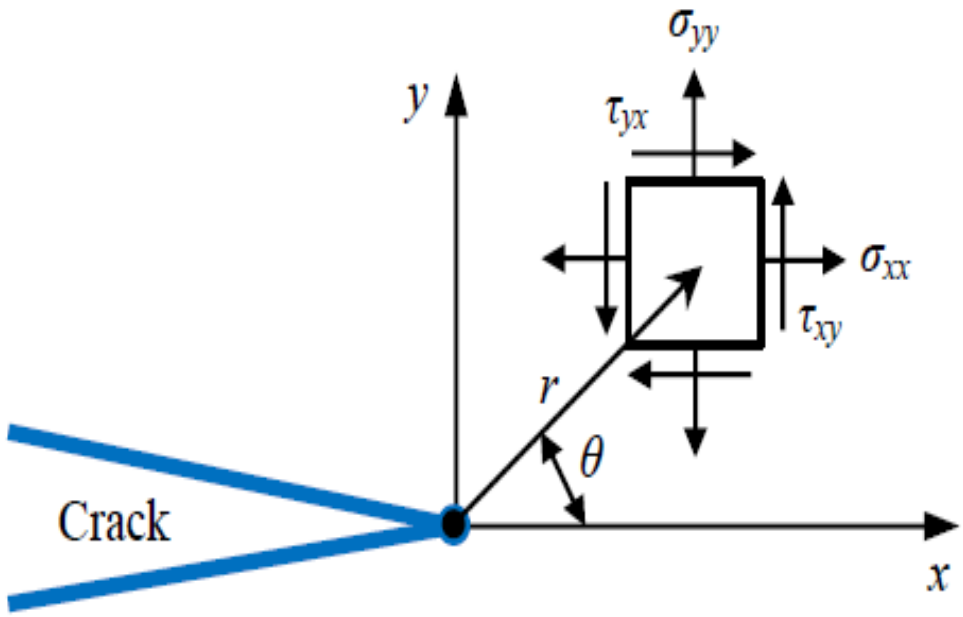

Figure 2. 5 Crack tip stress field [19]

$$\sigma_{ij}^{(I)} = \frac{K_I}{\sqrt{2\pi r}} f_{ij}^{(I)}(\theta) \tag{2.16}$$

$$\sigma_{ij}^{(II)} = \frac{K_{II}}{\sqrt{2\pi r}} f_{ij}^{(II)}(\theta) \tag{2.17}$$

$$\sigma_{ij}^{(III)} = \frac{K_{III}}{\sqrt{2\pi r}} f_{ij}^{(III)}(\theta) \tag{2.18}$$

Where the superscripts and subscripts *I*, *II*, and *III* denote the three different modes that different loadings may be applied to a crack. Usually interested in the maximum stress near the crack tip and whether it exceeds the fracture toughness. Thus, the stress intensity factor K is commonly expressed in terms of the applied stresses σ at $r \to 0$ and. $\theta = 0$ For linear elastic materials, the principle of superposition applies a mixed-mode problem can be treated as the summation of each mode.

$$\sigma_{ij}^{(TOTAL)} = \sigma_{ij}^{(I)} + \sigma_{ij}^{(II)} + \sigma_{ij}^{(III)} \tag{2.19}$$

2.3.4. Fatigue Crack Initiation

Crack initiation is a process that forms cracks on the surface of a material. The primary reason for the formation of cracks on any surfaces is fatigue. Fatigue leads to progressive and localized structural damage when any material experiences cyclic loading.

Cracks are often induced from so called non-metallic inclusions. An inclusion is any material that is trapped inside another material or just air bubbles inside a material. Around these inclusions the

stresses tend to be much higher than in the rest of the material and this is one reason for the initiation of cracks in these regions. According to Ekberg, pores seem to be one of the most dangerous types of material imperfections in railway wheels and according to the theory of elasticity; the shape of the defect will have a major influence [15].

Micro mechanical-based finite element framework is developed to investigate the effects of temperature change, traction coefficient, and grain size on initiation and progression of RCF. indicate that colder temperatures increase the progression of RCF, Large traction forces at the wheel-rail interface significantly accelerate RCF growth, Controlling the grain size can have a positive effect on both the initiation and migration of sub-surface cracks [2].

2.3.5. Fatigue Crack propagation

Fatigue cracks failure may start at free surfaces or internal (sub surface) in the material typical at the metallurgical imperfections creating areas with higher stress. And from External imperfection such as scratches from bad handling, deviation from machining, surface roughness, or a weakening due to temperature (welding).

The crack growth rate is described from the relation of change in crack length da and change in number of cycle's dN. In case of determining the lifetime of a structure subjected to a constant amplitude load-case, modification of the crack growth models from above is implemented [20].

$$N = f(da, \Delta k, R) \tag{2.20}$$

Therefore, the number of cycles to crack propagation was calculated using the crack growth models of Paris,

$$N = \frac{da}{C\Delta k^n} \tag{2.21}$$

When the stress and cyclic loading under the material increases the stress concentration in the weakened spot increases and the crack might grows with each cyclic load and expands to grow normal to max principal stresses. At last when the crack has grown large enough resulting in final fracture [21].

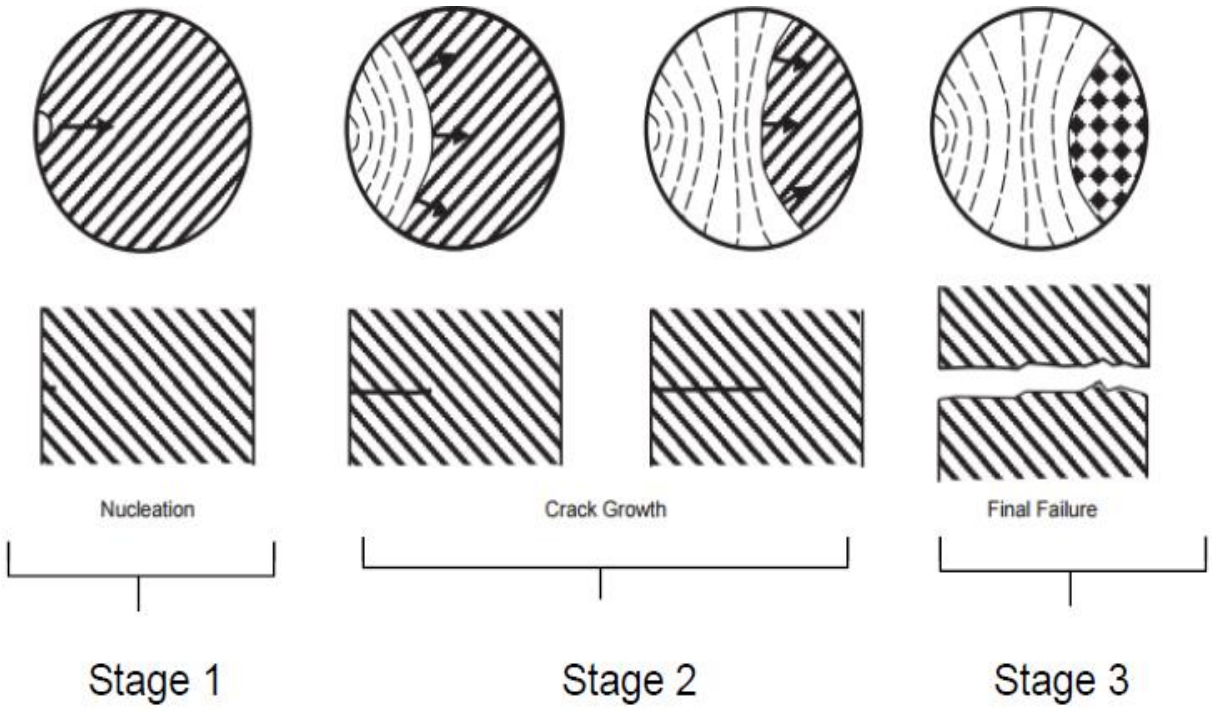

Figure 2. 6 Typical fatigue crack propagation [19][21]

Fatigue failure typically propagates in three steps.

1. Crack initiation: When the crack length becomes long enough the stress field at the crack tip become more dominant, so that the crack changes direction perpendicular to the principal stress, and the crack enters stage two.

2. Crack propagation: the crack proceeds to grow with the given pattern and path of fatigue striations. One striation will represent one load cycle and can be viewed in a microscope. Beach marks are created when the stress changes, for example during starting and stopping.

3. Fracture: Finale when fatigue crack becomes long enough that the remaining cross section no longer support the load. Final fracture happens sudden brittle and even for ductile materials.

2.3.5.1. Mixed mode crack propagation

Two types of crack propagation modes for a two-dimensional system are the tensile mode (K_I) and the shear mode (K_{II}). If K_{II} *is* zero the crack propagation can only be due to the remote tensile load and if K_I is zero or negative the crack propagation must be in the shear mode.

Hua *et al.* developed a way for express crack propagation under biaxial loading where finite K_{II}, and positive K_I, are both present at the crack tip. This corresponds to the so-called "mixed-mode" crack propagation regime, where neither K_I nor K_{II} individually represent the criteria for crack propagation [1].

Various modes of mixed mode crack propagation criteria have been proposed based on stress or energy method with Modified Griffith criterion, Maximum tangential stress (MTS) criterion and Strain energy density criterion

For modified Griffith criterion crack extension will occur in the direction where the total energy release rate is high and the extension will take place when the maximum energy release rate reaches a critical value. According to MTS criterion, the crack extension occur in the direction of tangential stress component at an infinitesimal radial distance and the extension take place when the maximum tangential stress reaches a critical value. Strain energy density criterion, crack extension will occur in the direction of minimum strain energy density reaches a critical value [17].

The SIF ranges be defined by the maximum and minimum SIF for each mode within each cycle

$$\Delta K_I = K_{I,max} - K_{I,min} \tag{2.22}$$

$$\Delta K_{II} = K_{II,max} - K_{II,min} \tag{2.23}$$

In order to determine the FCG for mixed mode loading by Paris law is an equivalent SIF required. A relationship based on the energy release rate is the equivalent SIF defined as [22].

$$\Delta K_{equ} = \sqrt{\Delta K_I^2 + \Delta K_{II}^2} \tag{2.24}$$

2.3.5.2. Mixed mode critical energy release rate

In some cases Fracture often occurs under a combination of modes, and so an equivalent critical value is required that the total energy release rate is the sum of the energy released from each mode, $G = G_I + G_{II} + G_{III}$ but this is not the case with the critical values. A universally accepted method for determining a mixed mode G_C does not exist, but appropriate method must be selected based on a relationship describing the mixed mode G_c calculations are available in Abaqus 6-13.3. The following mixed-mode G_c calculations are available in Abaqus 6-13.3. In 1984, Whitcomb used the superposition of stresses to develop a power law relationship describing the mixed mode delamination of composites during buckling assuming that Mode I and II are primarily responsible for delamination. One of the results from his report was.

$$\Delta G_C = \left(\frac{G_I}{G_{IC}}\right)^{\alpha} + \left(\frac{G_{II}}{G_{IIC}}\right)^{\beta} \tag{2.25}$$

Where α and β are empirically determined constants.

While testing glass/epoxy composites in 1996, Benzeggagh and Kaine observed that G_c increased as fracture transitioned from pure Mode I to pure Mode II. They developed the mixed Mode I-II,

semi-empirical criterion in a combination of the critical values based on the fraction of G_{II} present in the analysis. The exponent η is t to experimental data.

$$G_C = G_{IC} + (G_{IIC} - G_{IC})\left(\frac{G_{II}}{G_I + G_{II}}\right)^{\eta} \tag{2.26}$$

This was extended to three dimensions in 2006 by Reeder at NASA. The equation combines all three fracture modes and η_1 is an empirical constant. Reeder also concluded that Equation has no physical significance in two dimensions and thus should not be used in those cases.

$$G_C = G_{IC} + (G_{IIC} - G_{IC})\left(\frac{G_{II} + G_{III}}{G_I + G_{II} + G_{III}}\right)^{\eta_1} + (G_{IIIC} - G_{IIC})\left(\frac{G_{III}}{G_{II} + G_{III}}\right)\left(\frac{G_{II} + G_{III}}{G_I + G_{II} + G_{III}}\right)^{\eta_1} \tag{2.27}$$

2.3.6. Lubrication mechanism

The simulation of the surface crack propagation should also consider the influence of the lubricant on crack propagation. Several mechanisms and models have been proposed in the past.

a) The hydraulic pressure mechanism, where the lubricant is driven into the crack by contact loading pressure and keeps the crack faces separated by its pressure, thus implying increased modes I and II separation at the crack tip due to additional normal pressure and lack of friction between crack faces.

The fluid may be forced into the crack by the applied load and thus keep and separate the crack surfaces by its pressure (i.e. hydraulic pressure mechanism). In this case the crack propagates under mixed-mode conditions, where $K_I > K_{II}$ experimentally showed that this mechanism can cause steep crack propagation to the free surface.

b) Mode II crack propagation due to cyclic shear stresses along lubricated contacting crack surfaces, resulting in higher K_{II} values in comparison to dry crack surfaces.

c) The mechanism of trapped fluid, where the crack mouth closes under the contact pressure and the trapped fluid is driven toward the crack tip; this results in mode I separation at the crack tip, reduction of the crack face friction and increase in the mode II influence on crack propagation.

In the present computational procedure the hydraulic pressure mechanism has been adopted, where the lubricant pressure inside the crack is simply approximated with a uniform pressure distribution along the crack faces is considered to be equal to that at the crack mouth, in regard Friction between crack surfaces is assumed to be 0.04 for well lubricated contact in the numerical computations.

d) Multiple cavities could be completely or partially filled with lubricant and can join into a single cavity or get separated one from another (Kudish and Burris, 2004) [23].

2.3.6.1. Hydraulic pressure mechanism

The effect of hydraulic pressure mechanism model build-up inside the crack, was developed by Keer and Bryant the model is based on the assumption that the lubricant penetration is sufficient to fill the crack and The fluid may be forced into the crack by the applied load as the load rolls over the crack mouth when fluid inside the crack is pressurized by the contact load and thus separate the crack surfaces by its pressure (i.e. hydraulic pressure mechanism). In this case the crack propagates under mixed-mode conditions, where $K_I > K_{II}$ Kaneta and Murakami (1987) experimentally showed that this mechanism can cause steep crack propagation to the free surface. [23].

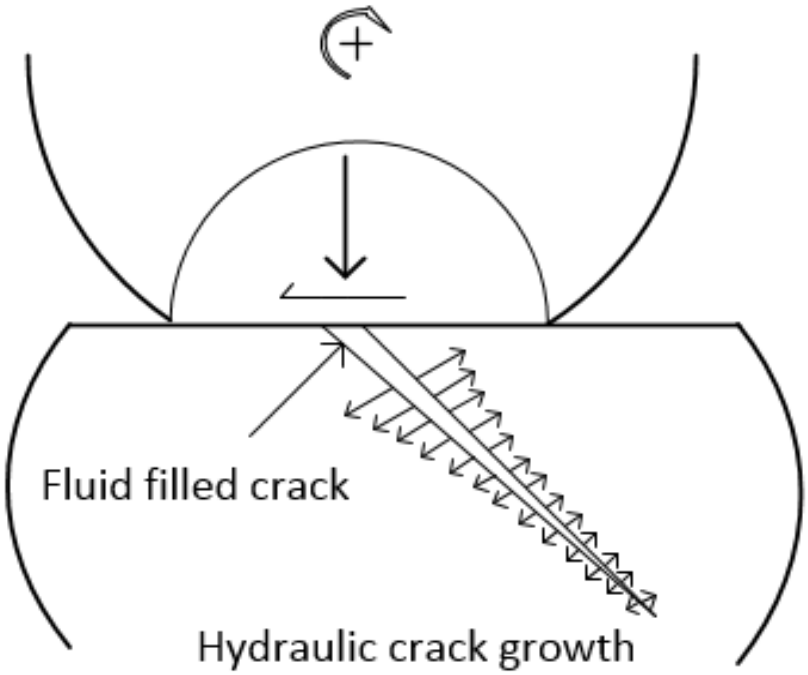

Figure 2. 7 Tensile model crack growth due to hydraulic transmission of contact pressure [23][24]

The pressure is equal to the Hertzian, or surface film pressure at the mouth and zero pressure at the tip. Have assumed a constant pressure within the crack, equal to the Hertzian or surface film pressure at the crack mouth.

2.3.6.2. Fluid entrapment mechanism

The Fluid may be trapped inside the crack when the mouth of the crack is closed and the fluid becomes sealed inside the crack by the contacting element unable to escape with the entrapped fluid is assumed to be incompressible at constant pressure.

The trapped fluid has two effects, firstly the fluid pressure can generate Mode I stress intensities as the fluid is forced towards the crack tip in which mode I propagation is more pronounced during the moving contact ($K_I > K_{II}$), secondly the fluid keeps part of the crack open and therefore reduces the resistance of the crack to shearing therefore also increasing the Mode II stress intensities. Experimental results showed that the trapped fluid inside the crack can cause crack propagation.

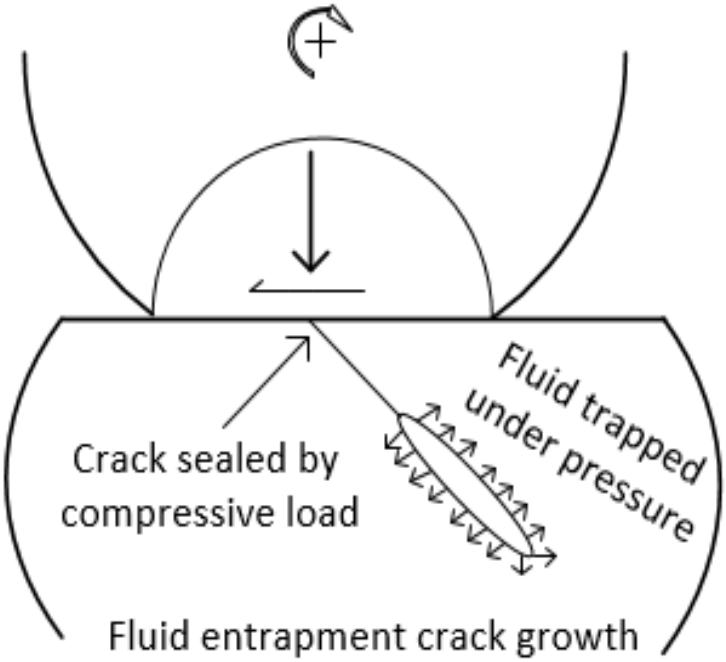

Figure 2. 8 Fluid assisted crack growth due to entrapment & fluid pressurization [23][24]

The present of lubricant between the mating bodies and inside the crack is taken into account and its effect on the crack is modeled via hydrostatic elements Suggest that the fluid pressure inside the crack produced by the fluid entrapment mechanism tend to those of the fluid pressurized as the crack become short [25].

2.4. Numerical Method

Abaqus is a suite of powerful engineering simulation programs based on the finite element Method, sold by Dassault Systèmes as part of their SIMULIA Product Life-cycle Management (PLM) software tools.

- Abaqus contains an extensive library of elements that can model virtually any geometry.
- May import geometry from a many different CAD software packages.
- Using Abaqus, be able to use various different material models to simulate the behavior of most typical engineering materials including metals, rubber, polymers, composites, reinforced concrete, crushable and resilient foams, and geotechnical materials such as soils and rock.
- Designed as a general-purpose simulation tool, Abaqus can be used to study more than just structural (stress/displacement) problems. It can simulate problems in such diverse areas as heat transfer, mass diffusion, thermal management of electrical components (coupled thermal-electrical analysis), acoustics, soil mechanics (coupled pore fluid stress analyses), and piezoelectric analysis.
- Abaqus offers a wide range of capabilities for simulation of linear and nonlinear applications. Problems with multiple components are modeled by associating the geometry defining each component with the appropriate material models and specifying component interactions. In a nonlinear analysis Abaqus automatically chooses appropriate load increments and convergence tolerances and continually adjusts them during the analysis to ensure that an accurate solution is obtained efficiently.
- Performing static as well as dynamic analysis (see both Abaqus/Standard and Abaqus/Explicit).

The methods used to apply LEFM to cracks with particular application to RCF problems can be divided into two main categories: those based on a boundary element approach and those based on a finite element approach. Numerical study of contact materials surface and sub-surface fracture under different mode are modeled with different approach, Boundary Element Methods (or boundary integral methods), Greens Function Method, Distributed Dislocations, Weight Function Method, Conventional finite element method and extended finite element method. The most widely used numerical approaches, and namely, conventional FEM and XFEM were used to model two dimensional crack propagation problems.

2.4.1. Conventional finite element method in abacus

For modeling crack propagation by means of conventional FEM, which is also called re-meshing technique approach, the crack should be modelled using embedded line, which is called “seam" in ABAQUS, at estimated location of initial crack. In order to model sharp crack propagation based

on conventional FEM technique two steps are important. The first step is capturing singularity at crack tip. For a sharp crack the stress field becomes singular at the crack tip. Including the singularity at the crack tip for a small-strain analysis improves the accuracy of the J-integral, Stress Intensity Factors and in general the stress and strain fields calculations. The second step is refining the mesh at each crack propagation increment. The re-meshing technique requires re-mesh the new model and crack tip after advancing the crack in each increment of crack propagation.

The application of this numerical technique to evaluate cracks however presents some problems. Regular finite elements are unable to accurately capture singular behavior at the tip of a crack in a LEFM type analysis, because the method is numerical and a near singularity leads to ill conditioning however some literature have developed ways to get around this problem by using two approaches First being the use of a high density of elements around the crack tip and secondly Use of a 'quarter point' node which can introduce a singularity of order $1/r$ on the side of the node at the crack tip. From this, the strain energy release rate and stress intensity factor can be calculated by extending the crack by a quarter of the length of the crack tip element size.

However fully numeric and singularities have traditionally led to ill conditioned matrices and inaccuracies. So, improvements in FEA, and commercial FEA software such as ANSYS and ABAQUS, are beginning to increase the applicability of FEA to crack modelling such as extended finite element method [26].

Minimization of contact stress as well as deformation to arrive at the best combination of driver and driven gear is recorded as aluminum and Developing FEM stress state fields in contact areas of teeth flanks, teeth fillets and parts of helical gears [27]–[29].

Artificial defect did not have a strong influence on crack initiation, but the height of the edge buildup, surface roughness, texture, hardness and temperature was the dominant parameter on surface crack initiation and fatigue life [30]–[32].

2.4.1.1. Contour integral

To model fracture mechanics of cracking in quasi-static problems using contour integral. The stress intensity factors can be calculated from the J-integral with the so called interaction integral method. The J-integral is a contour integral method to calculate the strain energy release rate, the energy dissipated during fracture per unit created fracture surface area.

The XFEM model together with the construction of the contour integral for SIF calculation, meshing techniques, simplification techniques and post-processing procedures.

On the basis of the relationship between the J-integral, stress intensity factors and the equivalent Young's modulus, E_c, May the energy released rate G for a general homogenous two-dimensional mixed-mode crack be expressed as [22].

$$J = G = \frac{K_I^2}{E_c} + \frac{K_{II}^2}{E_c} \tag{2.28}$$

$$E_c = \{ E \text{ plain stress}, \frac{E}{1 - v^2} \text{ plain strain} \tag{2.29}$$

Where E is Young's modulus and v is Poisson's ratio. Further are the J-integral specified The integral can described by path around the crack tip given with the following expression [20].

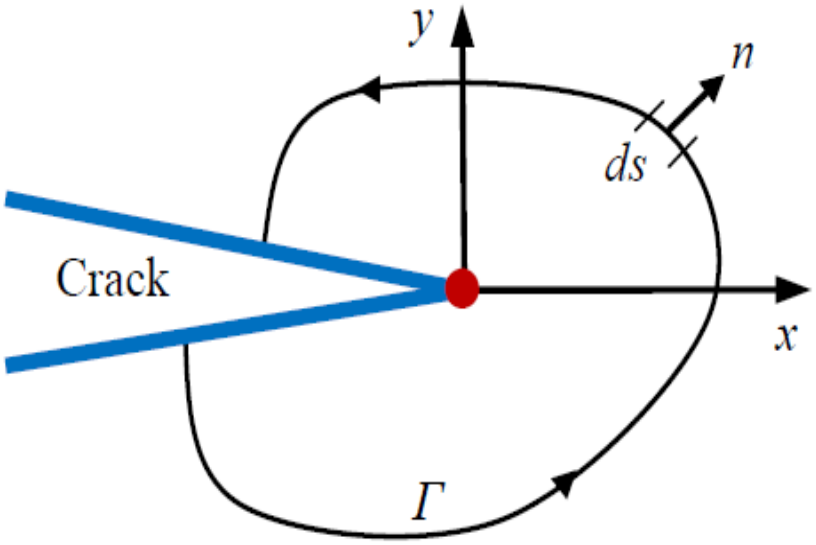

Figure 2. 9 Contour around the crack tip [19]

$$j = \int_{\Gamma}^{\cdot} \left(W_{n1} - \sigma_{jk} n_j \frac{\partial u_k}{\partial x_1} \right) d\Gamma \tag{2.30}$$

Where W is the strain energy density, σ is stress and u is displacement. To ease the implementation to a finite element code the equation should be rewritten by introducing the Dirac delta to the first term of the integral.

$$j = \int_{\Gamma}^{\cdot} \left(W_{\sigma_{1j}} - \sigma_{jk} \frac{\partial u_k}{\partial x_1} \right) n_j d\Gamma \tag{2.31}$$

To determine the mixed-mode SIFs are auxiliary stress and displacement set superimposed onto the XFEM displacement and stress state. The auxiliary displacement and stress states at the crack tip for a homogenous crack are calculated from the definitions established by Westergaard and Williams.

$$u_1^{(a)} = \frac{1}{2\mu}\sqrt{\frac{r}{2\pi}}\left[K_I \cos\frac{\theta}{2}(k - \cos\theta) + K_{II}\sin\frac{\theta}{2}(k + 2 + \cos\theta)\right] \quad (2.32)$$

$$u_2^{(a)} = \frac{1}{2\mu}\sqrt{\frac{r}{2\pi}}\left[K_I \cos\frac{\theta}{2}(k - \cos\theta) + K_{II}\sin\frac{\theta}{2}(k + 2 + \cos\theta)\right] \quad (2.33)$$

$$u_3^{(a)} = \frac{2}{\mu}\sqrt{\frac{r}{2\pi}}\left[K_{III}\sin\frac{\theta}{2}\right] \quad (2.34)$$

$$\sigma^{(a)} = \begin{bmatrix} \sigma_{11}^{(a)} & \sigma_{12}^{(a)} & \sigma_{13}^{(a)} \\ sym & \sigma_{22}^{(a)} & \sigma_{31}^{(a)} \\ sym & sym & \sigma_{33}^{(a)} \end{bmatrix} \quad (2.35)$$

$$\sigma_{11}^{(a)} = \frac{1}{\sqrt{2\pi r}}\left[K_I \cos\frac{\theta}{2}\left(1 - \sin\frac{\theta}{2}\sin\frac{3\theta}{2}\right) - K_{II}\sin\frac{\theta}{2}\left(2 + \cos\frac{\theta}{2}\cos\frac{3\theta}{2}\right)\right] \quad (2.36)$$

$$\sigma_{22}^{(a)} = \frac{1}{\sqrt{2\pi r}}\left[K_I \cos\frac{\theta}{2}\left(1 + \sin\frac{\theta}{2}\sin\frac{3\theta}{2}\right) - K_{II}\sin\frac{\theta}{2}\cos\frac{\theta}{2}\cos\frac{3\theta}{2}\right] \quad (2.37)$$

$$\sigma_{12}^{(a)} = \frac{1}{\sqrt{2\pi r}}\left[K_I \sin\frac{\theta}{2}\cos\frac{\theta}{2}\cos\frac{3\theta}{2} + K_{II}\cos\frac{\theta}{2}\left(1 - \sin\frac{\theta}{2}\sin\frac{3\theta}{2}\right)\right] \quad (2.38)$$

$$\sigma_{23}^{(a)} = \frac{1}{\sqrt{2\pi r}}K_{III}\cos\frac{\theta}{2} \quad (2.39)$$

$$\sigma_{13}^{(a)} = -\frac{1}{\sqrt{2\pi r}}\sin\frac{\theta}{2} \quad (2.40)$$

$$k = \begin{cases} \dfrac{3-\nu}{1+\nu} & \text{plain stress} \\ 3 - 4\nu & \text{plain strain} \end{cases} \quad (2.41)$$

Where r and θ are the polar coordinates from crack tip, μ is, ν is Poisson's ratio and k is Kosolov constant. The superposition of the auxiliary displacement, $u_{ij}^{(a)}$ and stress, $\sigma_{ij}^{(a)}$, states and the XFEM displacement, $u_{ij}^{(x)}$, and stress, $\sigma_{ij}^{(x)}$, states into equation 2.42 gives.

$$J^{(a+x)} = \int_{\Gamma}^{\cdot} \frac{1}{2}\left(\left(\sigma_{ij}^{(a)} + \sigma_{ij}^{(x)}\right)\left(\varepsilon_{ij}^{(a)} + \varepsilon_{ij}^{(x)}\right)\sigma_{1j} - \left(\sigma_{ij}^{(a)} + \sigma_{ij}^{(x)}\right)\frac{\partial\left(u_i^{(a)} + u_i^{(x)}\right)}{\partial x_1}\right)n_j d\Gamma \quad (2.42)$$

A more convenient way to determine the mixed-mode SIF values compared to the domain integral is the interaction integral which gives a more robust and actual results [20]. On the basis of

equation 2.43 can the interaction integral be obtained by separating the integral into XFEM state $J^{(x)}$, auxiliary state $J^{(a)}$ and interaction state $I^{(a,x)}$

$$J^{(a+x)} = J^{(a)} + J^{(x)} + I^{(a,x)} \tag{2.43}$$

The interaction integral is given by:

$$I^{(a,x)} = \int_{\Gamma} \left[W^{(a,x)} \sigma_{1,j} - \sigma_{ij}^{(a)} \frac{\partial u_i^{(x)}}{\partial x_1} - \sigma_{ij}^{(x)} \frac{\partial u_i^{(a)}}{\partial x_1} \right] n_j d\Gamma \tag{2.44}$$

$$W^{(a,x)} = \sigma_{ij}^{(a)} \varepsilon_{ij}^{(x)} = \sigma_{ij}^{(x)} \varepsilon_{ij}^{(a)} \tag{2.45}$$

Where W(a,x)is the interaction strain energy density. Finally are the divergence theorem used to convert interaction integral from a line integral to an area integral:

$$I^{(a,x)} = \int_{A} \left[\sigma_{ij}^{(x)} \frac{\partial u_i^{(a)}}{\partial x_1} - \sigma_{ij}^{(a)} \frac{\partial u_i^{(x)}}{\partial x_1} - W^{(a,x)} \sigma_{1,j} \right] \frac{\partial q_s}{\partial x_{jj}} dA \tag{2.46}$$

Where q_s is a smoothing function with a value of 1 inside the line integral and 0 (zero) outside the integral. In order to select the area for the integration integral must path-independency be considered. Normally are path independence achieved at a radius equal to three elements about crack tip [8].

By the same principle may an interaction integral also be obtained with the basis in equation The J-integral are then superimposed and separated to:

$$J^{(a+x)} = J^{(a)} + J^{(x)} + \frac{2\left(K_I^{(a)} K_I^{(x)} + K_{II}^{(a)} K_{II}^{(x)}\right)}{E_c} \tag{2.47}$$

$$I^{(a,x)} = \frac{2\left(K_I^{(a)} K_I^{(x)} + K_{II}^{(a)} K_{II}^{(x)}\right)}{E_c} \tag{2.48}$$

2.4.2. Extended Finite Element Method in abaqus

This method of crack analysis is in its infancy (it has only been developed in the last decade) but has shown promise to become a very powerful tool for the numerical investigation of fractured structures, with special applicability to the study of crack propagation The method is based on a modification to the existing FEMs [23]. Until recently, cracks had to be modeled as part of the structure's geometry. The extended Finite Element Method was developed in 1999 by Belytschko and Black where cracks could be defined arbitrarily, independent of the mesh. A second iteration of the XFEM was introduced in 2006 by Song, Areias, and Belytschko where Phantom Nodes (XFEM-PN) and a Level Set Method (LSM) were used to locate the crack. This method naturally

lends itself to fatigue crack growth, where a crack propagates along a solution dependent path, independent of the mesh [1].

The XFEM allows superposing geometric discontinuities such as cracks onto an existing FE mesh. The strain fields introduced by the discontinuities are accommodated by properly extending the set of shape functions of the elements affected.

If crack propagation is of interest, the limitations of the standard FEM are obvious, as the crack tip region requires re-meshing after every crack extension which forces a reassembly of the stiffness matrix.

Modeling stationary discontinuities, such as cracks, with the conventional FE method requires that the mesh conforms to the geometric discontinuities. Therefore, considerable mesh refinement is needed in the neighborhood of the crack tip to capture the singular asymptotic fields adequately. Modeling a growing crack is even more cumbersome because the mesh must be updated continuously to match the geometry of the discontinuity as the crack progresses.

A new approach to this problem is presented by the XFEM, which is based on the theory of hierarchical shape functions. With this method it is possible to generate cracks independent from an existing mesh by using discontinuous displacement shape functions for modeling the crack opening.

XFEM simulation were conducted in order to evaluate mode I and II stress intensity factors using Domain based interaction integral approach for cracks under cyclic contact rolling and rolling-sliding conditions These results show that the location of crack and loading have significant effect on the SIFs [33], [34].

For the purpose of fracture mechanics analysis, the enrichment functions typically consist of the near-tip asymptotic function that captures the singularity around the crack tip and a discontinuous function (also called jump, Heaviside or step function) that represents the jump in displacement across the crack line (in case of 2-D crack). Using the partition of unity concept, XFEM adds a priori knowledge about the solution in the FE area and makes it possible to model discontinuities and singularities independently of the mesh.

Two distinct types of damage modeling within an XFEM framework: Cohesive damage based and linear elastic fracture mechanics using virtual crack closure technique.

2.4.2.1. Virtual crack closure technique

In XFEM uses linear elastic fracture mechanics for crack growth simulation with or without initial crack. The strain energy release rate at the crack tip is calculated by virtual crack closure technique using the principle of LEFM states that the strain energy released when the crack is extended by some amount is the same as the energy required to close the crack with the same amount.

LEFM-based damage

- Based on linear-elastic fracture mechanics
- Uses the virtual crack closure technique (VCCT) for damage evolution
- Specify damage initiation as part of the material definition such as Max principal stress criterion similar to CZM approach.
- Damage evolution and stabilization are specified as part of the interaction property definition to the XFEM crack.

2.4.2.2. Cohesive zone based damage model

The concept of a cohesive zone has been started by Dugdale (1960) and Barenblatt (1962) were the first to apply the concept of a cohesive stress zone to fracture modeling. Needleman (1987) recognized that cohesive elements are particularly attractive when interface strengths are relatively weak compared to the adjoining materials.

The cohesive behavior can be: Element-based Modeled with cohesive elements and Surface-based Modeled with contact pairs in Abaqus/Standard and general contact in Abaqus/Explicit. This kind of damage model approach uses XFEM based on traction separation cohesive behavior to model crack initiation and propagation using phantom nodes which are superimposed to the original node to represent the discontinuity of cracked element.

Cohesive damage

- Based on cohesive damage mechanics
- Uses traction-separation laws for damage initiation and evolution
- Damage properties such as initiation and evolution are specified in the material definition

Cohesive segment approach uses traction-separation laws. And it follows the general framework for surface based cohesive behavior. This method can be used for brittle and ductile materials. The material properties define the evolution of damage leading to eventual failure. The material is to the section that is assigned to the crack domain.

In the traction-separation laws, the normal traction stress vector includes two or three components, which depends on dimensions. Choosing to associate a normal behavior contact interaction property with the XFEM crack that defines the contact of cracked element surfaces. To assist the convergence as the material fails, localized damping can be introduced using the viscous regularization technique

For the cohesive segments approach there are three stress based criteria and three strain based criteria, they are maximum principal stress (MAXPS), maximum principal strain (MAXPE), maximum nominal stress (MAXS), maximum nominal strain (MAXE), quadratic nominal stress (QUADS), and quadratic nominal strain (QUADE). Crack initiation based on the stress/strain value at the center of enriched elements (Du).

Maximum nominal stress (MAXS) critical value

$$\mathrm{MAX}\left\{\frac{[\sigma_n]}{N_{max}}\ \frac{\sigma_t}{T_{max}}\ \frac{\sigma_s}{S_{max}}\right\} = f, \quad [\sigma_n] = \begin{cases}\sigma_n \text{ for } \sigma_n > 0\\ 0 \text{ for } \sigma_n < 0\end{cases} \tag{2.49}$$

Maximum nominal strain (MAXE) critical value

$$\mathrm{MAX}\left\{\frac{[\varepsilon_n]}{\varepsilon_n^{max}}\ \frac{\varepsilon_t}{\varepsilon_t^{max}}\ \frac{\varepsilon_s}{\varepsilon_s^{max}}\right\} = f, \quad [\varepsilon_n] = \begin{cases}\varepsilon_n \text{ for } \varepsilon_n > 0\\ 0 \text{ for } \varepsilon_n < 0\end{cases} \tag{2.50}$$

Damage initiation and damage evolution

The XFEM analysis requires material information in the enriched area of crack. The maximum principal (‘Maxps Damage’ in ABAQUS) was selected for the damage initiation criteria. The ultimate stress/strength was used as the limiting maximum principal stress. Damage evolution was based on an energy criteria which is equivalent to the strain energy release rate (‘Fracture energy’ on ABAQUS), G_I and a linear softening, maximum degradation a Mode independent.

For modeling the artificial crack propagation in Abaqus both damage initiation and damage evolution must define the criteria available. For damage initiation, the maximum principal stress criterion will be used where Damage will initiate when the maximal principal stress exceeds the Maxps. Damage initiation is defined as part of the material properties, using a traction-separation law Maxps.

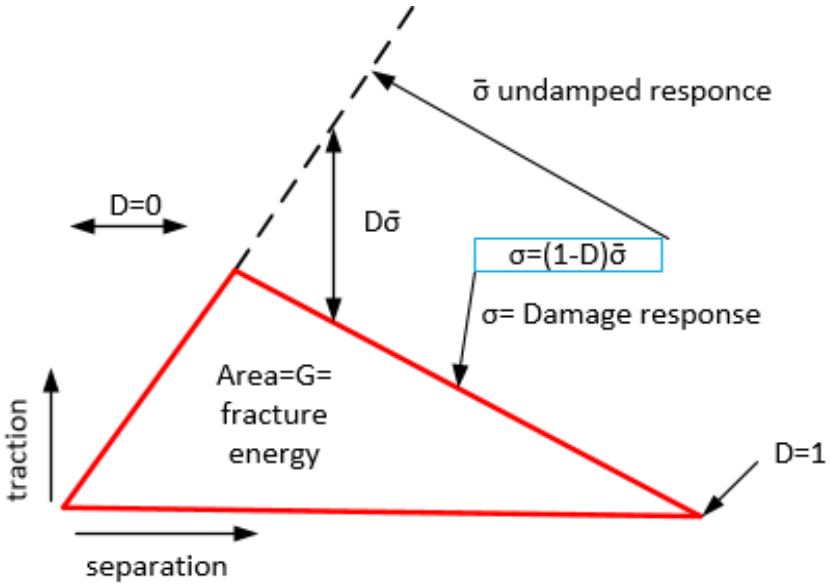

Figure 2. 10 Traction separation law

Once specifying damage initiation, defining how the material changes due to damage. In Abaqus, damage is modelled using a scalar damage parameter, D. This can range between 0 (no damage) and 1 (complete failure) [35].

Disc to disc contact models with initial crack are investigated. Results of using an extended finite element with linear elastic fracture mechanics and cohesive segment .Therefore it is possible to solve different engineering problems in complex domains, which may be practically impossible using classical FEM to solve. And XFEM has a great potential in computational fracture engineering problems than classical FE.

Interpolation scheme of Xfem

$$u = \sum_{i=1}^{N} N_i(x)\left[u_i + H(x)\alpha_i + \sum_{i=1}^{4} F_a(x) b_i^a\right] \tag{2.51}$$

Where: u = displacement vector

N_i = shape function

u_i = nodal displacement vector

$H(x)$ = jump function

α_i = nodal enriched degree of freedom vector

$F_a(x)$ = asymptotic crack tip function

b_i^a = nodal enriched degree of freedom vector

In the above XFEM displacement function Equation (2.51), asymptotic function and jump function are used for fracture analyses. In the XFEM method, there are three strain criterions and three stress criterions. In the study of XFEM, the maximum principal stress criterion is used as the evaluation factor of the material properties. For the VCCT method, it is based on the quantity of strain energy released when the crack is extended.

Asymptotic Crack-tip Function

In case of not completely cracked element, the Heaviside function cannot be used to approximate the displacement field over the entire element domain, since the element contains the crack tip.

The tip function is given by:

$$F_a(x) = \left[\sqrt{r}\sin\frac{\theta}{2}, \sqrt{r}\cos\frac{\theta}{2}, \sqrt{r}\sin\theta * \sin\frac{\theta}{2}, \sqrt{r}\sin\theta * \cos\frac{\theta}{2}, \right] \quad (2.52)$$

Where (r, θ) is the polar coordinate system with its origin at the crack tip

Jump Function

Shape function applies to all nodes in the model while Jump function applies to nodes, whose shape function cut by the crack interior and asymptotic crack-tip function applies to node whose shape function support is cut by the crack tip in two-dimensional problems, crack modelling is obtained by means of two different types of enrichment functions:

The Heaviside function H(x), is employed to enrich elements completely cut by the crack. The splitting of the domain by the crack, causes a jump in the displacement field and the Heaviside function provides a tremendously simple mathematical tool to model such behavior.

The jump function can be written as Equation which is support cut by crack interior.

$$H(x) = \begin{cases} 1, & \text{if } (x - x_1).n \geq 0 \\ -1, & \text{other wise} \end{cases} \quad (2.53)$$

Where,

x = sample (gauss) point

x_1 = the closet point to x on the crack

n = unit outward normal to the crack at x_1

(a) Smooth crack. (b) Kink crack.

Figure 2. 11 Evaluation of the Heaviside function

A node being enriched by both the Heaviside function and crack tip enrichment features

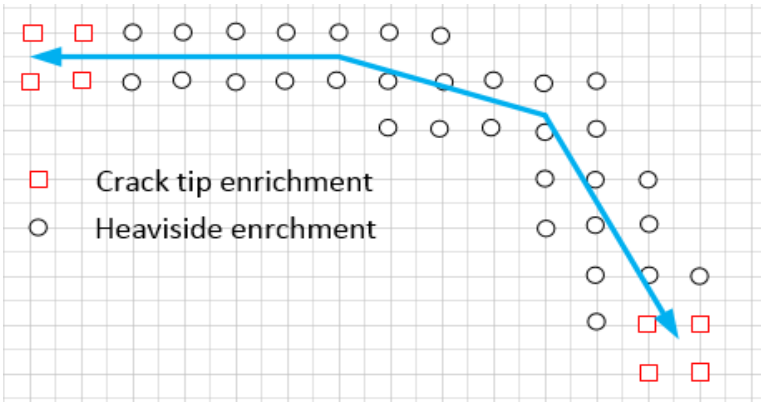

Figure 2. 12 Enrichments in the XFEM [15]

Level set method for modeling discontinuities

Enriching finite element approximation with the asymptotic near-tip field and the Heaviside function H(x) in the enrichment scheme can be solved crack growth problems with minimal re-meshing. Mostly, the numerical simulations of objects vary with time, like curves and surfaces on a fixed Cartesian coordinate grid, e.g. interfaces, discontinuities, etc. Their modelling and tracking is based on the complex mathematical procedure denominated parametrization and XFEM capabilities can be extended in conjunction with the Level Set Method (LSM) allows to get over these difficulties. The key-point of such method is to represent discontinuities as a zero level set function and characterize a crack, with two different level set functions to represent the crack position and location of crack tips

$$\varphi = (\mathrm{x} - \bar{x}).\mathrm{n}. \tag{2.54}$$

Where x and n assume the previously stated above.

Whether a node lies above or below the crack, simply needs to retrieve sign of Ψ at a point. If the crack cuts through an element, then $\Phi \leq 0$ and $\Psi_{min}\,\Psi_{max} \leq 0$, where Ψ_{min} and Ψ_{max} are the minimum and maximum values of Ψ at that point. Nodes of this element are enriched with discontinuous jump function. If crack tip lies inside an element, then, $\Phi_{min}\,\Phi_{max} \leq 0$ and $\Psi_{min}\,\Psi_{max} \leq 0$, and nodes of the element are enriched with crack tip enrichment function [19].

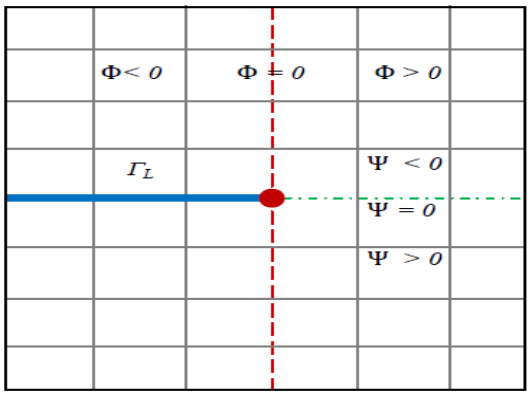

Figure 2. 13 Construction of level set function [27]

2.5. Related Papers

N. Govindarajan and R. Gnanamoorthy [36] Finds the theoretical contact fatigue life of sintered and hardened steel under various contact conditions results equivalent stress for sintered and hardened steels is approximately 3.2 times higher than that of AISI 4340 pore free steels for the same contact conditions. C. Santus, M. Beghini, I. Bartilotta, and M. Facchini [37] tried to distinguished RCF into subsurface initiated (spalling and case crushing) and surface initiated (pitting and micro pitting). The characteristic depths and the stress index approach can be used to relate specific tests to component design, without any size effect misinterpretation.

G. Fajdiga [8] investigates parameters such as High contact pressures, small contact surface curvatures, high friction, and high tensile residual stresses, high mean velocities of contacting surfaces and high kinematic viscosity have a negative influence on the stress distribution.

S. Tesfaye, A. Molinari, and W. Pahl [6] deals with lubricated rolling-sliding behavior of a gas carburized 0.85%Mo and 0.3%C sintered steel and the effect of shot peening were studied. Formation of contact fatigue cracks at the Hertzman depth and surface cracks due to tensile stresses was theoretically and experimentally investigated. S. T. Mekonone, W. Pahl, and A. Molinari [10] studied sintered and sinter hardened condition investigate for possible effect of the microstructural heterogeneity, density and sintering time on both the subsurface fatigue crack nucleation and the surface plastic deformation results sintering time for the high density steels was twice than sintered

ones**.** S. Marble [38] developed Mixed lubrication model to include rough surfaces in a transient elliptical contact under rolling/sliding conditions for a Newtonian lubricant demonstrates heat generated due to asperity friction and consequent flash temperature rise in the contact zone. P. Purushothaman and P. Thankachan [39] Fatigue was investigated numerically for single asperities Suggests that asperity point contacts can create sufficiently large tensile stresses for fatigue in the lubricated contacts even without slip**.**

Z. Golmohammadi, A. Walvekar, and F. Sadeghi [40] Develop a 3D efficient elastic-plastic finite element model to characterize the rolling contact fatigue behavior of hardened steel at high loads includes the effects of variation of contact pressure and residual stresses due to the plastic deformation**.** D. Hannes and B. Alfredsson [41] Influence of friction and the crack inclination angle on the damage spread in the contact surface. Both low crack inclination angles and increased friction resulted in larger spall opening**.**

W. Pu, D. Zhu, J. Wang, and Q. J. Wang [42] Investigate the critical effect of relative sliding motion on contact fatigue life, due to the increased number of stress cycles and the high asperity contact pressure, for concentrated contacts in mixed lubrication without considering wear leads in accelerated pitting**.** J. Jurenka and M. Španiel [43] Complex parametric FE model, advance cavity model, methodology for implementation of residual stress into subsurface layers for pitting crack growth was created based on Paris' phenomenological approach.

F. Li, W. Hu, Q. Meng, Z. Zhan, and F. Shen [44] used Numerical simulations of crack initiation, crack propagation, and spalling are performed Results that fatigue damage before the crack initiation mainly affects the magnitude of the contact stresses and not the shape of their distribution but damage in the crack propagation stage influences both the magnitude of the contact stresses and the shape of their distribution**.**

O. Slávik, P. Hutař, M. Berer, A. Gosch, F. Arbeiter, [3][45] develops Numerical procedure to predict the rolling contact fatigue crack initiation in wheel- crossing to obtain stress and strain results, and mixed mode loading conditions for understanding damage of polymer bearings results in form of the SIFs, describes fatigue crack.

M. Bozkurt, A. O. Ayhan, and M. F. Yaren [46] FEM and experimental studies on a mode-I/III are presented by changing the loading holes with contact mechanics show that the mode-II SIF change sign along the crack front and their magnitudes are close to the mode-III SIF. Mode-III SIF do not vary much along the crack front**.** R. Citarella and M. Perrella [47] Effects of specimen

complex geometry, on fracture crack path are analyzed under mixed mode conditions and SIF are determined.

T. He [48] analyze an efficient method for simulating PEHL MODEL in a rolling contact and has been compared with the previous PEHL model shows that computational speed of the present model is greatly increased, high as about four times Investigate the critical effect of relative sliding motion on contact fatigue life, due to the increased number of stress cycles and the high asperity contact pressure, for concentrated contacts in mixed lubrication without considering wear leads in accelerated pitting.

J. Flas, B. Zafos, and R. Potoc [49] Simulation of a surface initiated fatigue crack growth under rolling and sliding contact conditions assuming that the initial crack of length initiated at the surface due to previous mechanical or heat treatment, taking into account the influence of the SIF K_I and K_{II}, T-stress, stress on the crack surface caused by lubricant pressure inside the crack and critical distance ahead of the crack tip. Investigate the contribution of surface roughness; friction and a constant residual surface to the RCF damage process and initiation, crack path and fatigue life were examined for a gear application. FEM and analytical method is similar with minimum variations [5].

C. Klaassen, A. Crawford, A. K. Prathuru, and R. Gordon [50] Characterize the failure behavior of metal-to-metal effects by varying adhesive type (ductile or brittle), quality of bond (adhesive contact area) and mode-mixity of the specimens were investigated using mixed mode bending test and simulated using FEM.

R. Vijaywargiya and I. Green [51] FEA results of sliding between two elastic–plastic bodies in cylindrical contact explores deformations, forces, stress formations, and energy losses for frictionless and friction sliding contact**.** P. Bocher [52] shows the effects of induction hardening on RCF studied using FEA introducing residual stress and hardness gradients. Residual tensile become a limiting factor for fatigue rolling contact life**.**

S. Ancellotti, M. Dallago, and V. Fontanari [53] uses numerical technique to estimate the effect of lubricant, inclination angle, the friction coefficient between the mating surfaces, the half-width, and the maximum intensity on the Stress Intensity Factors of inclined edge cracks under rolling-sliding fatigue. During the first propagation stages fluid entrapment does not affect the SIFs, but when the crack size increases the crack deviate from its original trajectory.

2.6. Summery

Many researchers go through cracking formation and propagation of rolling sliding mechanical components failure under different parametric conditions. The effect of lubricant, inclination angle, friction coefficient, surface roughness, High contact pressures, small contact surface curvatures, high tensile residual stresses, high mean velocities of contacting surfaces and high kinematic viscosity between the mating surfaces on fracture crack path are analyzed under different modes of conditions.

Even though several researches were carried out on the numerical methods to determine the contact parametric effects. Mixed Mode Surface Fracture of sintered pre alloyed carburized 0.85% Mo and 0.3% C porous sintered steel material subjected to contact load has not been studied numerically yet.

This thesis work has got the value of filling the gap of considering cracks induced at the carburized surface studying the propagation of the crack under the effect of compressive mechanical load, friction and lubrication pressure effect using an efficient mathematical formulation found in ABAQUS known as extended finite element method.

Chapter Three: Methodology

3.1. Material

The materials constituting the bodies in contact can differently deform to the applied stresses. The kind of response depends on the applied force, the properties of the materials' involved, and the geometry of the bodies in contact. The most important materials' properties are the elastic properties, such as the longitudinal modulus of elasticity and Poisson's ratio, the yield strength, hardness and fracture toughness.

The paper describes a computational simulation of the crack growth starts from the initial surface crack because of the material porosity. The proposed model is based on a 2-dimensional plane strain crack propagation analysis, where the required material properties are obtained from micro hardness (HV0.1) tests [10].

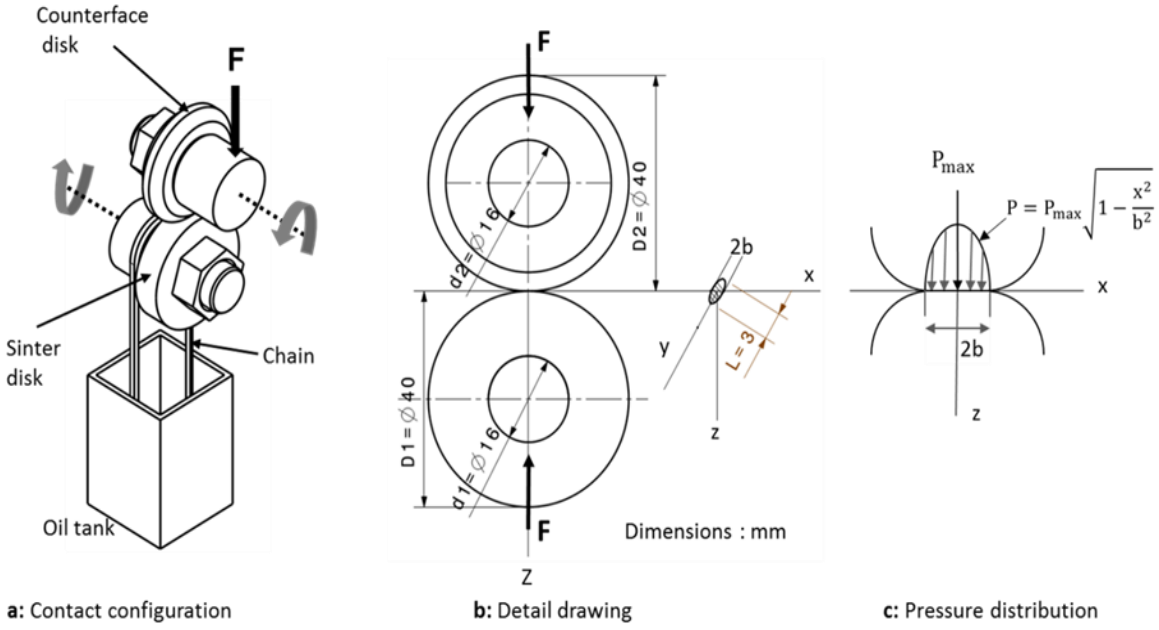

a: Contact configuration **b:** Detail drawing **c:** Pressure distribution

Figure 3. 1 Configuration, drawing & pressure distribution (cylinder axis along y-axis) [6]

Lubricated rolling-sliding tests were carried out on disk to disk configuration using Amsler tribometer machine with Master disc act as driver while the Slave discs is driven (follower disc). Figure 3.1 represents the schematic tribometer setup of contact configuration, detail drawing of sinter disk and counter face disk (was machined to reduce contact length). All the analysis of Hertzman contact pressures and stress of pearlitic steels were used in these tests were made using their material compositions, dimensions and properties of two contacting materials as given in Table 3.1.

Table 3. 1 Dimensional characteristics

Parameters	Sinter disk	Counter face disk
L [mm]	3	3
R1/R2 [mm]	20	20
Rpm	360	400

Assumptions

- Since the material is porous crack can initiate anywhere else in the sintered disc
- The material modelling problem (Even though for the carburization case that varies its property in the depth direction) assume to take an average mean value
- Mesh convergence is done for determining the contact stress only not for the crack analysis
- 2D plain strain condition

3.2. Fracture toughness

Fracture toughness can be defined as the ability of materials to resist fracturing and propagation of pre-existing cracks or is the fracture energy consumption rate required to create new surfaces. K_{IC} can be used to predict failure for different combinations of stress and crack size and for different geometries and so K_{IC} can be considered a material property characterizing the crack resistance, and is therefore called the plane strain fracture toughness.

An approach is to perform a series of different experiments and reach at a critical stress intensity factor K_c for each material, this critical parameter when measured under certain conditions is known as the fracture toughness [54]. The fracture toughness can be expressed as a function of crack extension is called the resistance curve shows the Variation in fracture toughness with crack growth. Fracture toughness and material property values of materials and sintered steel types are listed below.

Table 3. 2 Material property

Parameters	Sinter disk	Counter face disk
σ_y	720 MPa	-
E1/E2	155 GPa	210 GPa
ν_1/ν_2	0.27	0.3
K_{IC}	$27MPa\sqrt{m}$	-

3.3. Fracture modelling tool

Abaqus is powerful computer-aided engineering simulation software and is a suite of powerful engineering simulation programs, which is designed for model generation, data analysis, results evaluation, and visualizing the FEA results based on the finite element method that provides a simple, consistent interface for creating Abaqus models, interactively submitting and monitoring Abaqus jobs, and evaluating results from Abaqus simulations.

Finite element analysis can resolve both simple linear problems and most nonlinear simulations as well. Abaqus contains a large number of geometric elements library, which can simulate various kinds of geometries. Moreover, Abaqus contains a variety of material models, which could be used to define the behaviors of those materials. Designed as a general-purpose simulation tool, Abaqus can be used to investigate more than just structural (stress/displacement) problems; it can simulate problems under the condition of diverse areas such as heat transfer, mass diffusion, thermal management of electrical components (coupled thermal-electrical analysis), acoustics, soil mechanics (coupled pore fluid-stress analyses), piezoelectric analysis, electromagnetic analysis, and fluid dynamics.

Abaqus offers a wide range of capabilities for simulation of linear and nonlinear applications. Problems with multiple components are modeled by associating the geometry defining each component with the appropriate material models and specifying component interactions. In a nonlinear analysis system, Abaqus automatically selects appropriate load increments and convergence tolerances and continually adjusts them during the analysis to ensure that an accurate solution is efficiently obtained.

A fracture analysis typically starts with an initial crack size, or crack initiation criteria based on stress or strain, and propagates the crack until a critical value is reached such as K_C or G_C.

3.3.1. Methods of Fracture Analysis

Predicting the crack growth trajectory and to evaluate the SIF under mixed modes (I & II) using numerical method. Finite element mesh is generated using a singular elements to facilitate the crack process, the fracture analysis and J integral was employed to evaluate the SIFs under mixed mode loading conditions for capturing the stress intensity factor and crack propagation determining using XFEM. So that, the accuracy of both SIF`s values and the crack growth path predictions results are compared and validated with relevant published research work [6].

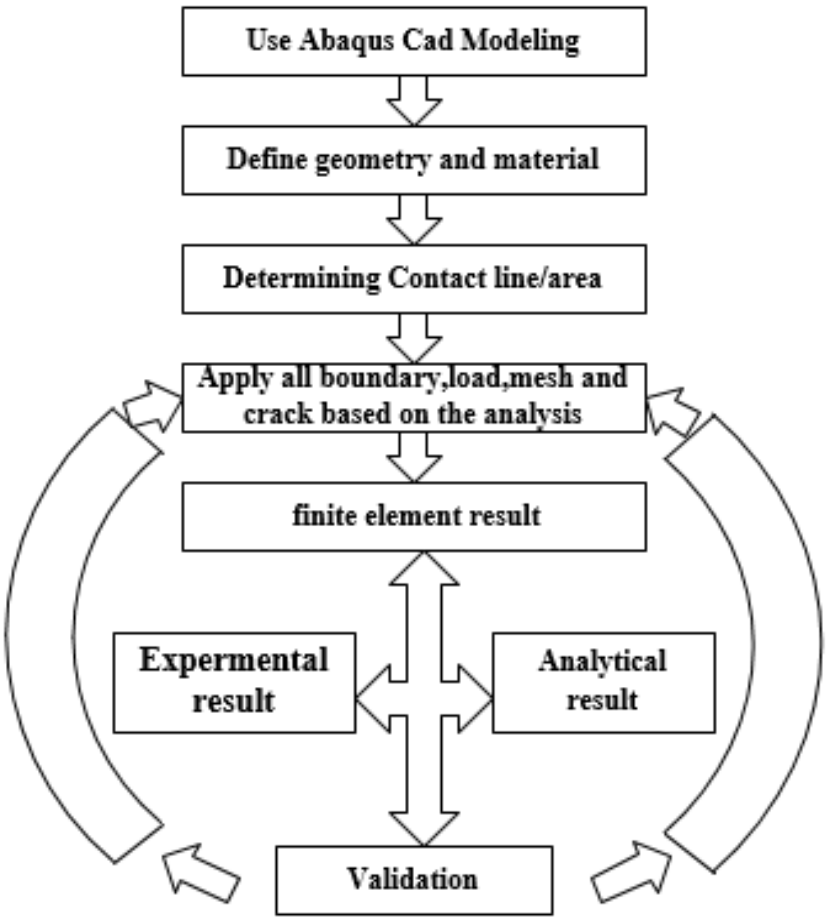

Figure 3. 2 Numerical methodology analysis

This study model the crack propagation of disc to disc contact by using XFEM and Crack growth for different coefficient friction in terms of friction between the crack face and lubrication pressure along the crack face with Cohesive zone modeling approaches are investigated.

The essential background about XFEM with both cohesive segments approach, virtual crack closure technique approach based on linear elastic fracture mechanics approach and, for simulation of damage of crack.

A fracture analysis typically starts with an initial crack size, or crack initiation criteria based on stress or strain, and propagates the crack until a critical value is reached such as K_c or G_c. Growth rates are calculated using a fatigue crack growth model such as the Walker.

Extended finite element method to predict the fracture direction of propagation within a specimen, and to compute the stress intensity factor for cracked plates under different loading conditions. Using the maximum energy release rate criterion and interaction integrals.

To be able to compute cracks using XFEM in Abaqus, a few simple steps are needed; a crack must be defined, the crack domain must be chosen, the enrichment radius is defined and the output of interest is specified. These steps are explained below according to Abaqus 6.11 Online Documentation [55].

Crack is created as a wire surface for 2D cases and positioned as desired. Abaqus automatically finds the positioning of the crack in the solid model using the Level set method. The Level set method defines the crack using isoplanes; defines the crack face and defines the crack front and is orthogonal to. The isoplane is called PHILSM in Abaqus and needs to be selected in the Field output requests to be able to visualize the crack opening in the post-process.

The crack domain defines where the enrichment features can be added to the finite element approximation, i.e. the region where a crack can be described with XFEM. It is specified manually and for stationary crack analyses it must contain any existing crack.

The enrichment radius is a radius from the crack tip and defines in which element nodes the crack tip functions are added. It can be manually chosen or Abaqus calculates the radius as three times the typical element characteristic length. This characteristic length is a typical length of a line across an element. The radius is chosen to be calculated automatically in all models presented in the stationary crack evaluation.

The last step is to specify the number of contours to be included in the contour domain to calculate the stress intensity factors. The parameter controls the number of element rings around the crack tip that construct the contour domains for the contour integral calculation).

3.3.2. Crack Modelling

Initiation crack

In the common fracture mechanics representation, cracks are modelled as discontinuities possessing smooth and frictionless surfaces. A simple equivalent hertizian contact model is used for simulating the fatigue crack propagation under a given initial crack conditions of rolling and sliding contact as described in the fig 3.3.

The contact model is subjected to normal compressive contact force and friction between the contact rolling discs, which also take into account the influence of lubrication conditions in terms of pressure between the initial crack surfaces. The surface initial crack is angled in the opposite direction of the acting frictional forces or direction of rolling as the experimental orientation.

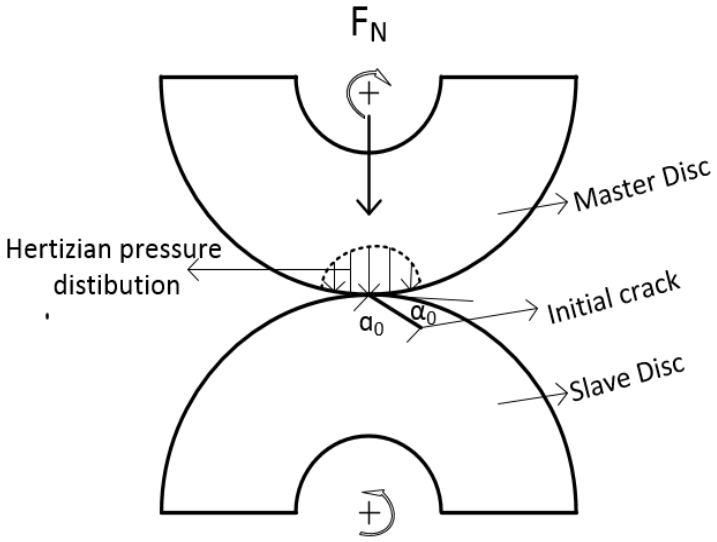

Figure 3. 3 Orientation of initial crack under compressive loading

The compressive contact pressure acting in the z-plane at the contact remains almost constant, so it can be analyzed with a reasonable degree of accuracy in 2D using the plane strain condition approximation. In rolling/sliding contact fatigue, it is known that the crack propagates at a characteristic angle 15°-30° to the surface [20][25].

Since the material is porous crack can initiate anywhere and the position of given initial crack located at the mid-point on the outer surface of the slave disc, of the contact, with that the initial length of the crack is equal to a_o=10 μm, and initial inclination angle towards the contact surface equal to $\alpha_o = 25°$. This positioning of the crack achieves the most frequently occurring initial cracks appearing on rolling sliding mechanical contact mechanisms of porous material.

For the purpose of the crack propagation simulation, XFEM method in the framework of the FEM has been applied. It is assumed that the crack will propagate in the direction that maximizes the release of the strain energy, resulting in the minimum possible total potential energy of the system.

This developed model has been used for the simulation of crack growth on two contact disc in plain strain condition. Porous Slave disc made of 0.85%Mo and 0.2%C sintered steel with Young's modulus $E = 1.55* 10^5$ N/mm^2 with Poisson ratio of ν=0.27 and master disc of $\nu = 0.3$ with $E = 2.1* 10^5$ N/mm^2. The maximum contact pressure P_{max}= 1210 N/mm^2 acts at the point of contact of the disc with the equivalent radius of disc R^* = 10 mm. the coefficient of friction $\mu = 0.04$ has been used, which is the average value for well-lubricated between the crack face [49].

The fracture energy can be defined as a function of mode mix using a tabular form or other form using BK (Benzeggagh-Kanane)

$$G_{IC} + (G_{IIC} - G_{IC})\left(\frac{G_{Shear}}{G_T}\right)^{\eta} = G_{TC} \quad (2.55)$$

$$\text{Where, } G_{shear} = (G_{II} + G_{III})$$

$$G_T = (G_I + G_{Shear})$$

For isotropic failure $G_{IC} = G_{IIC}$, the response is sensitive to the value of η

$$G_{IC} = \left(K_{IC}{}^2\left(\frac{1-\upsilon_1{}^2}{E_1}\right) + K_{IIC}{}^2\left(\frac{1-\upsilon_2{}^2}{E_2}\right)\right)$$

$$G_{IC} = \left(27^2\left(\frac{1-0.3^2}{210000}\right) + 30.3^2\left(\frac{1-0.27^2}{210000}\right)\right)$$

$$G_{IC} = 7.66\,{}^{N}/_{mm}$$

Then, the total critical energy release for mixed mode is given by eq. (2.55):

$$G_{TC} = G_{IC} + (G_{IIC} - G_{IC})\left(\frac{G_{II} + G_{III}}{G_I + G_{II} + G_{III}}\right)^{\eta}$$

$$G_{TC} = 7.66\frac{N}{mm} + \left(7.66\frac{N}{mm} - 7.66\frac{N}{m}\right) + \left(\frac{7.66\frac{N}{m}}{7.66\frac{N}{mm} + 7.66\frac{N}{mm}}\right)^{0.7}$$

$$G_{TC} = 8.27\,{}^{N}/_{mm}$$

The equivalent young's modulus of different property material is given according to the eq. (2.11)

$$\frac{1}{E_C} = \frac{1-\nu_1^2}{E_1} + \frac{1-\nu_2^2}{E_2}$$

$$\frac{1}{E_C} = \frac{1-0.3^2}{210000} + \frac{1-0.27^2}{155000}$$

$$E_C = 96{,}950.895\,{}^{N}/_{mm}$$

The equivalent radial dimension of the contact disc according to the eq. (2.12)

$$\frac{1}{R_C} = \frac{1}{R_1} + \frac{1}{R_2}$$

$$\frac{1}{R_C} = \frac{1}{20} + \frac{1}{20}$$

$$R_C = 10\text{mm}$$

The contact width of the master and slave disc at equivalent parameter and compressive load of 475 N is calculated based on the eq. (2.10)

$$b = \sqrt{\frac{4 * 10\text{mm} * 475}{\pi * 1 * 96{,}950.895}}$$

$$b = 0.25\ mm$$

$$2b = 0.50\ mm$$

Maximum contact pressure at the center of contact width of the disc is given with formula eq. (2.9)

$$P_{max} = \frac{2 * 475}{\pi * 0.25 * 1}$$

$$P_{max} = 1208.3\ \text{MPa}$$

The average contact pressure is given with eq. (2.8)

$$P_0 = 0.78 * P_{max}$$

$$P_0 = 1208.3\ \text{MPa}$$

For the contact compressive force F=362N $2b = 0.44mm$

$$P_{max} = 1047.53\ \text{MPa}$$

$$P_0 = 817.07\ \text{MPa}$$

For the contact compressive force F=293N, $2b = 0.40\text{mm}$

$$P_{max} = 940.6\ \text{MPa}$$

$$P_0 = 733.67\ \text{MPa}$$

Units System in ABAQUS

Abaqus doesn't specify a unit system, the user could use a unit system arbitrarily, as long as they are in consistency in the analysis problem made [56]. Author uses consistent basic units in abaqus.

Table 3. 3 System unit in abaqus

Parameter	Units
Force/load	Newton (N)
Displacement	millimeter (mm)
Mass	Tone (10^3 kilogram)
Time	Second (S)
Stress	MPa (N/mm^2)
Energy	mJ (10^{-3})
Density	$Tonne/mm^3$

3.3.3. Modelling Lubricant pressure effect

The effect of friction reduction model provides a simple way to model the lubricant in the crack but offers little towards a better understanding of the way that the crack deforms and propagates under the coupled effect of the lubricant penetration and contact loading [23].

The following assumptions are made in formulating the problem:

1. The model obeys linear elasticity
2. The crack surface and outer surfaces are perfectly smooth
3. The problem can be modelled in 2D using the plane strain assumptions
4. The crack has a stress singularity at the tip (no blunting is explicitly introduced)

When lubricant enters towards crack, the lubricant may coat the surfaces and form a lubricant film reducing the friction coefficient between the cracks faces this can in turn increase the shearing displacement of the crack faces and the shearing at the crack tip. So when we reduce friction we assume that apply shearing.

The cracks may be growth due to the action of fluid by fluid entrapment or with a form of lubricant pressurization was proposed and suggest that fluid is forced into the crack by the load as it rolls over the crack mouth, and then the faces of the cracks are exposed to fluid pressure so that this pressure acts to open the crack in a mode one type and generates a large build-up of stress intensity at the crack tip [23].

Many experimental studies have shown that lubricant must be present for contact fatigue, such as pitting, to occur in rolling systems and that without a lubricant, rolling contact fatigue is greatly reduced. So, that it is important to take into consideration this mechanism effect of interaction correctly interpreted and incorporated into a fracture mechanics model of rolling contact fatigue.

Fluid lubricated crack faces in which the lubricant reduces the friction between the crack faces and it does not exert pressure inside the cavity.

Fluid forced into the crack by the load that consists in applying on the crack faces a linear pressure distribution in correspondence of the crack mouth, such pressure is equal to the contact pressure between the two mating bodies, and equal to zero on the crack tip.

Fluid Entrapment Mechanism in which the fluid is assumed to be blocked by the mating body therefore the volume of fluid entrapped is kept constant into the cavity during the passage of the body $P_{max}=P_{crack}$ [25].

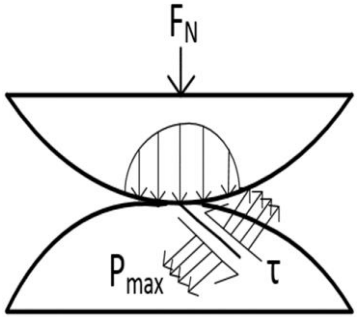

Figure 3. 4 Opening mode crack growth accelerated by pressure of the lubrication and shear mode crack growth with reduction of friction between the crack face

3.4. Procedure

3.4.1. Building the model

Two-dimensional model Finite element analysis offers many ways to analyze structures. It requires an understanding of the program and the characteristics of the object. Element types included shell and solid, wire elements can be used. The shell type can be take the form of linear or quadratic shape. These types have been considered and their results were compared. The creation of the model has been carried out through several steps. The first step is the drawing of the part using ABAQUS/CAE package where the part was considered as a planar deformable body with a shell base. The simulation has been carried out under the condition of isotropic material for both of the master disc and slave disc with linear-elastic fracture mechanics. Where the slave is fixed in all direction for displacement and rotation and the master disc fixed in the X direction for displacement and rotation and free rotation along the z axis. The applied load (radial load) acts the master disc vertically in the negative Z-direction.

Among the different element families, continuum or solid elements can be used to model the widest variety of components. Conceptually, continuum elements simply model small blocks of material in a component. Since they may be connected to other elements on any of their faces, continuum elements, like bricks in a building or tiles in a mosaic, can be used to build models of nearly any shape, subjected to nearly any loading.

The distribution of the maximum equivalent von Mises stress under the contacting area is first determined for pure Hertzian contact conditions, where the maximum stresses appear at a certain depth under the contacting surface. For computational simulations of non-conforming contact of mechanical elements it is advantageous to use a substitute model of two contacting cylinders instead of simulating the actual contact.

The substitute contact model of two cylinders can be transformed into equivalent contact model by utilizing the Hertzian contact theory. The equivalent contact model consists of a simple cylinder of equivalent radius and material properties along with applied standard Hertzian contact conditions.

3.4.2. CAD model module

In ABAQUS there is a drawing feature Part module used to define the geometry of the various interacting solids which makes it possible to draw the parts.

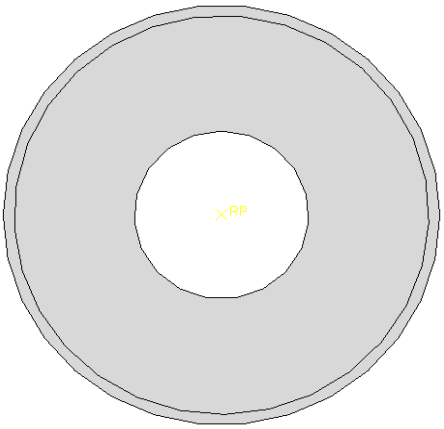

Figure 3. 5 Master disc modelling

Table 3. 4 Dimension of master roller disc

Part	Outer diameter	Inner diameter	thickness
Master disc	40mm	20mm	unity
Slave disc	40mm	20mm	unity

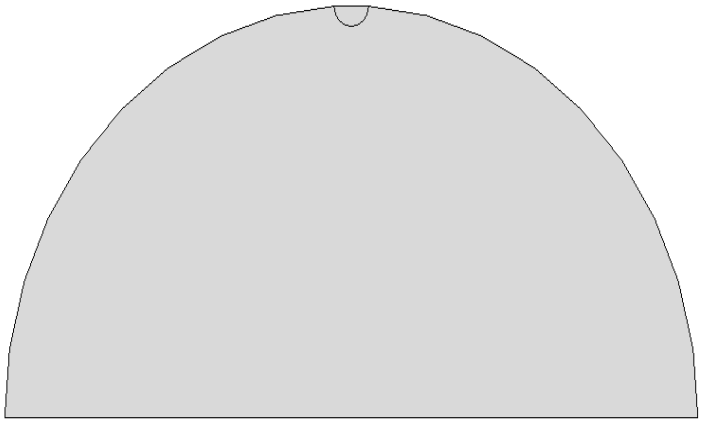

Table 3. 5 Equivalent model of slave disc

Table 3. 5 Dimensional of slave disc

Part name	Modeling space	type	Feature shape	Feature type
Master disc	2D	Deformable	Solid	Planer
Slave disc	2D	Deformable	Solid	Planer

3.4.3. Property module

The property module different material properties and body sections are assigned to specified regions of the master and slave disc. The master disc and slave disc consists of same material behavior, type and section type. Both the master and the slave disc of deformable body had a 40mm outer radius and 20mm inner radius. A two-dimensional, 4-node (bilinear), plane strain quadrilateral, reduced integration element (CPE4R), hourglass control was used.

Table 3. 6 Dimensional and material characteristics of master and slave disc

Part name	Material behavior	type	Young modules	Poisson's ratio	Section type
Master disc	elastic	isotropic	210000 MPa	0.3	Solid, homogenous
Slave disc	elastic	isotropic	155000 MPa	0.27	Solid, homogenous

3.4.4. Assembly module

This section illustrates development of basic contact modeling utilizing Abaqus for creating the instances of parts and positioning the instances relative to each other in a global coordinate system and modifies the assembly. The model contains only one assembly, which composed of instances of parts (master and slave disc) from the model and are assembled in the assemble module.

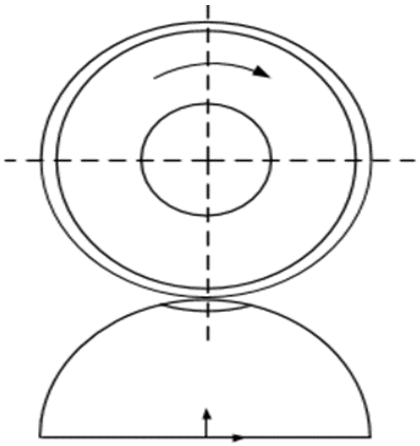

Figure 3. 6 Assemble model of master slave disc

3.4.5. Steps module

The step module creates different type of steps for analyzing and useful to make single steps for each change in the model. In every step can be prescribed what the output parameters have to be. Also the length of the step, the actual simulation time can be set. As well as the start, minimum and maximum value of a single increment and the maximum number of increments. In the initial step the model is checked or it is modeled in a correct way and if the output requests that are requested for each step are possible. In the first step the force is applied at the center point of hollow master disc. A ramp function is used to apply the force. In the second step this force is maintained and the disc starts to rotate with a prescribed speed. The length of this step determines the length of the path at the disc.

- Two steps analysis method was adopted to remove the load variation in the initial state
- Used abacus standard instead of abaqus explicit to avoid elastic wave and vibration noise in stress distribution result
- Step time does not matter in result because of the nature of steady state analysis
- Increment size should adjust so as to capture the exact solution of all analysis within the range of convergent step time

Table 3. 7 Static module analysis parameter

Step	Step name	procedure	Time period	Increment size			Max. number of increments
				initial	minimum	maximum	
0	initial	initial	N/A	N/A	N/A	N/A	N/A
1	Apply force	Static, general	1	0.1	0.0001	0.1	100
2	Rotation	Static, general	100	0.05	0.0001	0.005	10000

3.4.6. Interaction module

Surface-to-surface contact interactions describe contact between two deformable surfaces or between a deformable surface and a rigid surface. A surface-to-surface contact definition can be used as an alternative to general contact to model contact interactions between specific surfaces in a model. Certain interaction behaviors can be defined only by using surface-to-surface contact. The penalty of friction was included in the contact pair to define the friction behavior of the contact region. And can define contact between edges of a wire or between faces of a solid or shell. Certain connectivity restrictions apply to contact surfaces depending on the type of contact formulation.

Table 3. 8 Interaction property of master and slave disc

Interacting part	Interaction type	Contact property	Normal behavior	Contact formulation	Coefficient of friction
Master with slave disc	Surface to surface	Tangential behavior	Hard/soft contact	penalty	[0, 0.05, 0.1, 0.15, 0.2, 0.25, 0.3]

3.4.7. Loads and constraints module

The model is concentrated nodal forces applied to the displacement degrees of freedom Loaded in Z direction at the center of master disc as shown in figure 2.1. To be able to simulate the master slave simulation it is important that the BC's (Boundary Condition) are chosen in a proper way. Therefore the center node movements in the X stand Y direction are suppressed and rotations around the Z axis vector is free as well and the simplified slave disc is fixed at the bottom in all directions.

Table 3. 9 Load condition

Load type	location	Load at step 1	Load at step 2
Concentrated force	At the center of master disc	[475,362, 293] N	propagated

3.4.8. Mesh module

The new XFEM method permits to eliminate the limitations of the classical finite element method (FEM). This method makes possible to study the problems of crack propagation without re-meshing. In addition, the second advantage of this method is that the mesh of the structure is independent of the crack geometry, this is feasible with new enrichment functions that allow dealing with the problem of the singularity at the point of the crack that is, to overcome the problem of the singularity at the point of the crack tip and the discontinuity of the displacement.

A two-dimensional, 4-node (bilinear), plane strain quadrilateral, reduced integration element (CPE4R) used. The mesh size of 0.02 mm *0.02mmm was considered at contact interface and decreased gradually far from the contact region for all models. This mesh size was gained by mesh convergence study. The finite element mesh generated by choosing the meshing technique that ABAQUS/CAE use to create the mesh, the element shape, and the element type with different number of meshing techniques for the best consistence mesh refinement by seeding the edge of the part to appropriate element size.

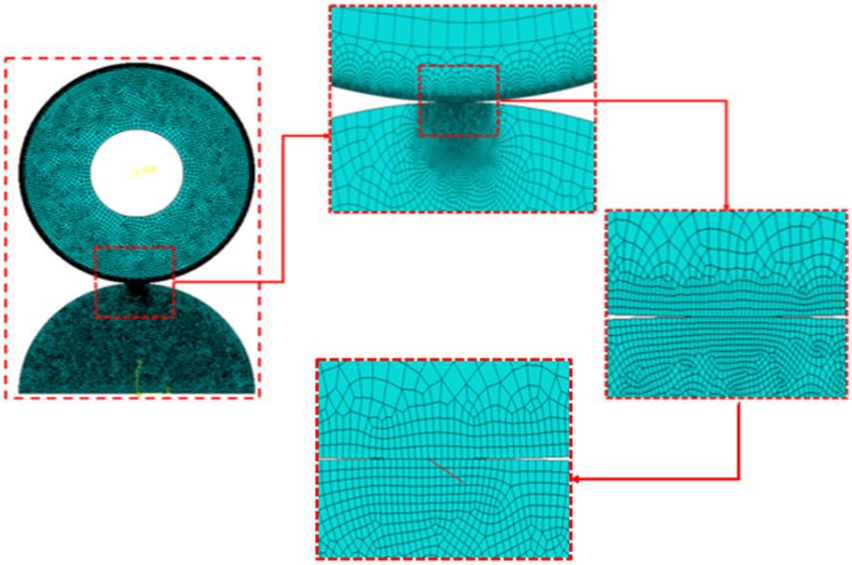

Figure 3. 7 The finite element mesh shown in has been used in subsequent analyses.

3.4.8.1. Convergence analysis

Different solutions can be adopted while meshing a master slave disc for equivalent stress. The mesh size at contact interface should be fine to capture the relaxed stress state near the contact between the master and slave disc surface. In order to do mesh convergence study to find a mesh size which produce correct results, the modelling with mesh refinement was continued until an appropriate convergence of the stress state was achieved without using too many elements which increase calculation time. The study uses maximum von-misses stress and is set up with average elements size from 1mm to 0.02 mm.

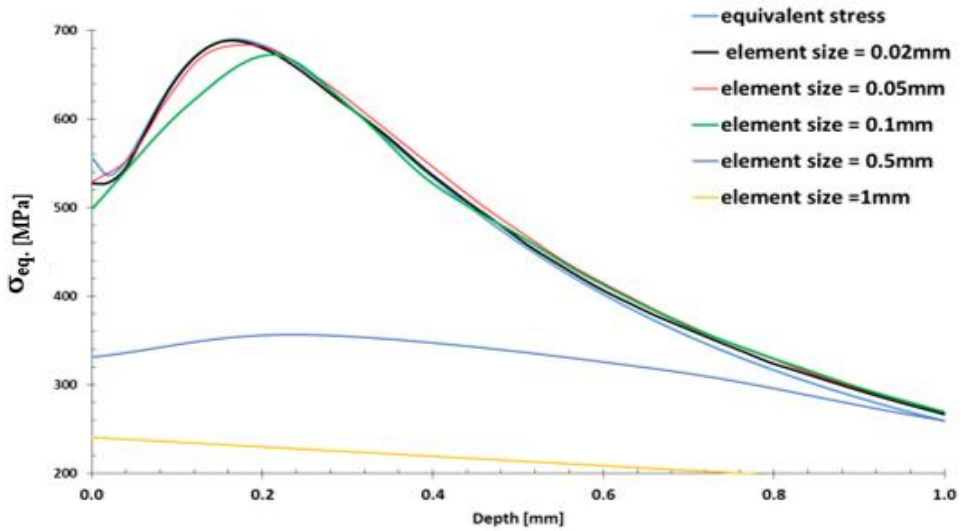

Figure 3. 8 mesh convergence analysis

The local mesh convergence analysis at the contact surface is done for determining the exact result of contact stress and contact pressure not for the crack growth since extended finite element is used for crack analysis which is independent of mesh.

Table 3. 10 Parameter of mesh convergence

Mesh no	Local Mesh element size	Number of elements	Numerical Equivalent stress	Hertizian equivalent stress	Processing time in (sec)
1	0.02	57652	688.87	690	19680
2	0.05	21894	683.62	690	5420
3	0.1	10073	672.60	690	2715.7
4	0.5	4573	356.43	690	1247.2
5	1	1362	240.65	690	337

According to mesh convergence study results, an acceptable element size was determined to be at least less than 0.02mm in the refined contact zone

Table 3. 11 Mesh property of master slave disc

	Element type	Element library	Geometric order	family	Element size
Master	CPE4R	standard	linear	Plain strain	0.02mm
Slave	CPE4R	standard	linear	Plain strain	0.02mm

3.4.9. Job Module

Having finishing all of the tasks involved in defining a model (such as defining the geometry of the model, assigning section properties, and defining contact), using the Job module to analyze the model and allows to create a job, to submit it for analysis, and to monitor its progress.

3.4.10. Visualization Module

This module shows all the output requested in terms of graphical display of finite element model and result Plot Contours on deformed Shape and un deformed shape, contours, graphs, animations of analysis with respective visualization variable value and animation scale factor.

Chapter Four: Result and Discussion

4.1. Finite element method results

4.1.1. Influence of applied load on Von Mises stress and pressure distribution

The most influential parametric factors of contact surfaces are the initial crack length, crack angle, contact force, friction and the hydraulic pressure of fluid acting on the crack face surfaces. In this paper the effect of applied load and coefficient of friction is shown on:

a) Von Mises stress distribution

b) Pressure distribution

The equivalent computational model used in the figure 2.2 with a given data used for determining the maximum Von Mises equivalent stress and its position, depth *Z* under the contact surface, have been computed for different compressive contact load at a friction coefficient μ=0.3

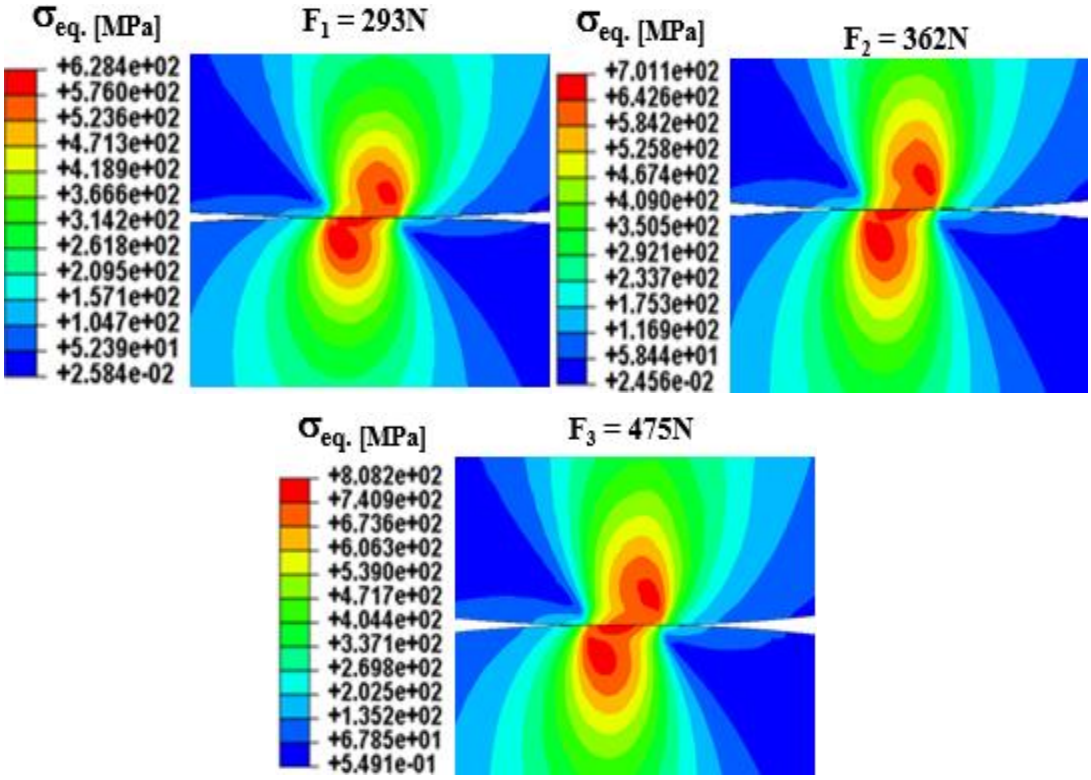

Figure 4. 1 The effect of load on equivalent Von Mises mechanical stress with μ=0.3

Based on the Hertzian contact theory, the contact equivalent Von Mises stress for variable load magnitude condition is calculated using finite element method Abaqus. From the above result figure 4.1 shows that the Von Mises equivalent stress increases with the increase of the load to maximum Von Mises stress.

The equivalent mechanical Von Mises stress along the depth with different compressive contact force is simulated and verified at the contact.

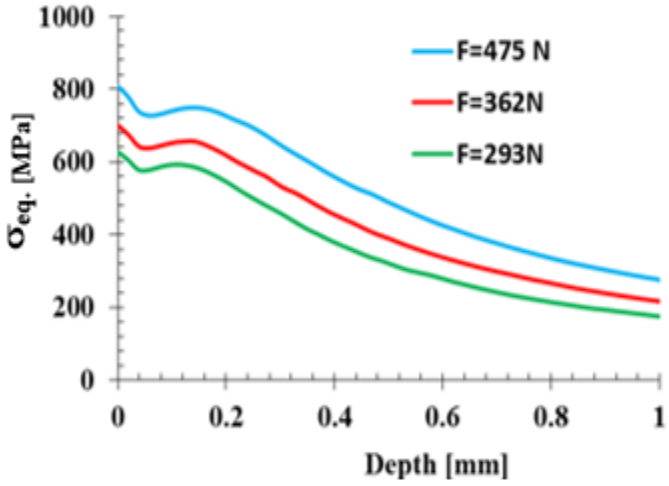

Figure 4. 2 The effect of load on mechanical equivalent Von Mises stress along depth

Figure 4.2 shows that when the load increases the equivalent mechanical Von Mises stress along the given 1mm depth decrease. Similarly, the effect of load on the contact pressure distribution were determined in figure 4.3 represents the contact pressure at compressive load of 475N, 362N and 293N respectively with μ=0.3

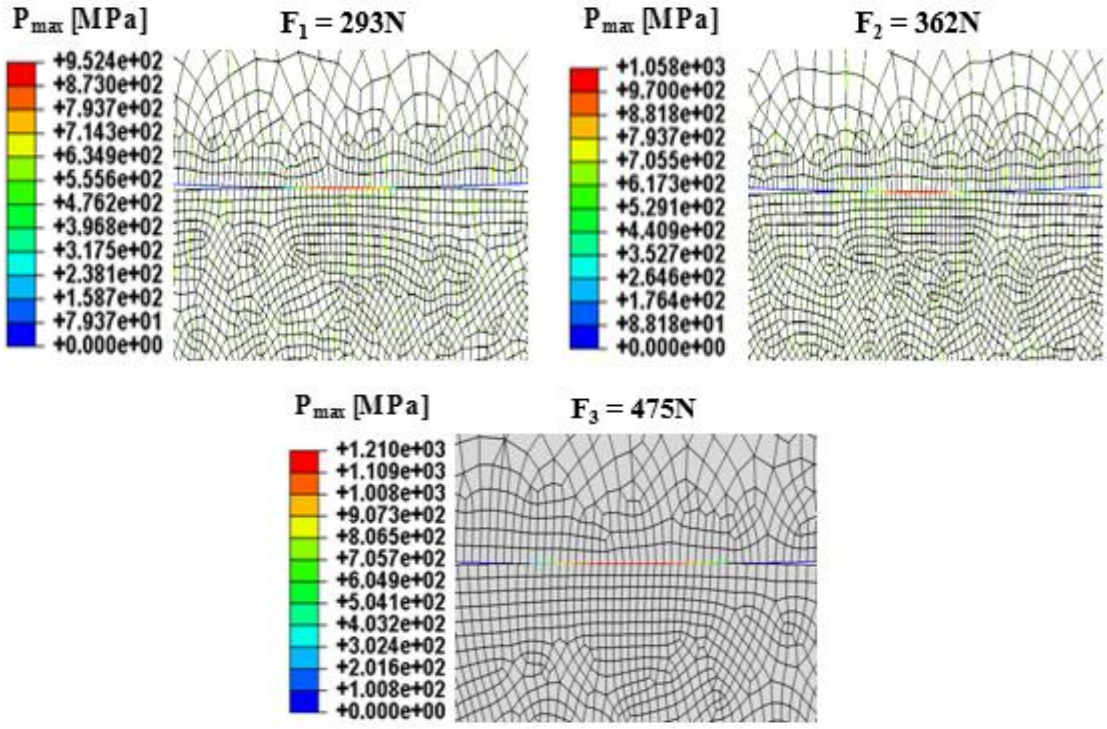

Figure 4. 3 Effect of load on contact pressure

The model result shows that increasing of maximum pressure with load. The results obtained from the finite element model verify that the relation between the contact pressure and the applied load are in comparison with the analytical results [as reported in method section].

The contact pressure and the contact width with different contact force is simulated. Figure 4.4 represents the effect of load on pressure distribution and contact width.

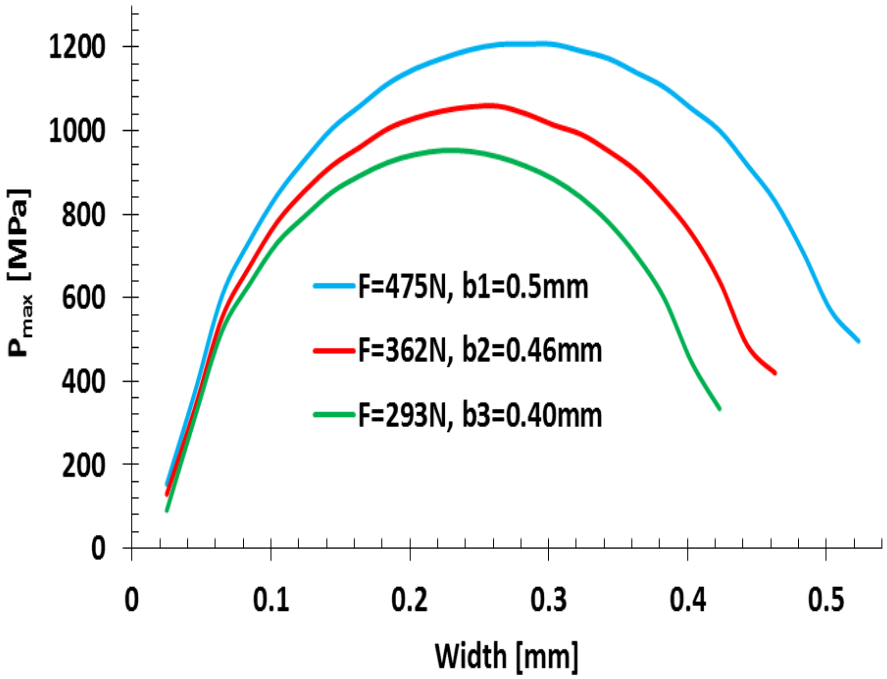

Figure 4. 4 The effect of load on contact pressure along width of contact

The maximum pressure and contact width increases with contact load. At 475 N load, maximum pressure and contact width are 1210 MPa and 0.5mm, respectively.

Table 4. 1 Von Mises stress & contact pressure using hertzian theory and FEM analysis

	Von Mises stress Value (MPa)	Contact pressure (MPa)
Fem value	687.5	941.64
Hertzman value	690	950
Error (%)	0.34	0.88

4.1.2. Influence of contact friction coefficient on Von Mises stress and pressure distribution

The effect of contact friction parameter on the contact surfaces of rolling sliding mechanical elements usually transmit a certain tangential traction forces. The influence of these friction on the Von Mises equivalent mechanical stress of the rolling sliding disc mechanical elements is evaluated numerically using abaqus CAE and abaqus standard.

Contact equivalent Von Mises mechanical stress can be simulated in its simplest form by applying the compressive load and friction, where the distribution of frictional contact loading *q(x)* can be easily determined from the normal loading *P(x)* and coefficient of friction μ.

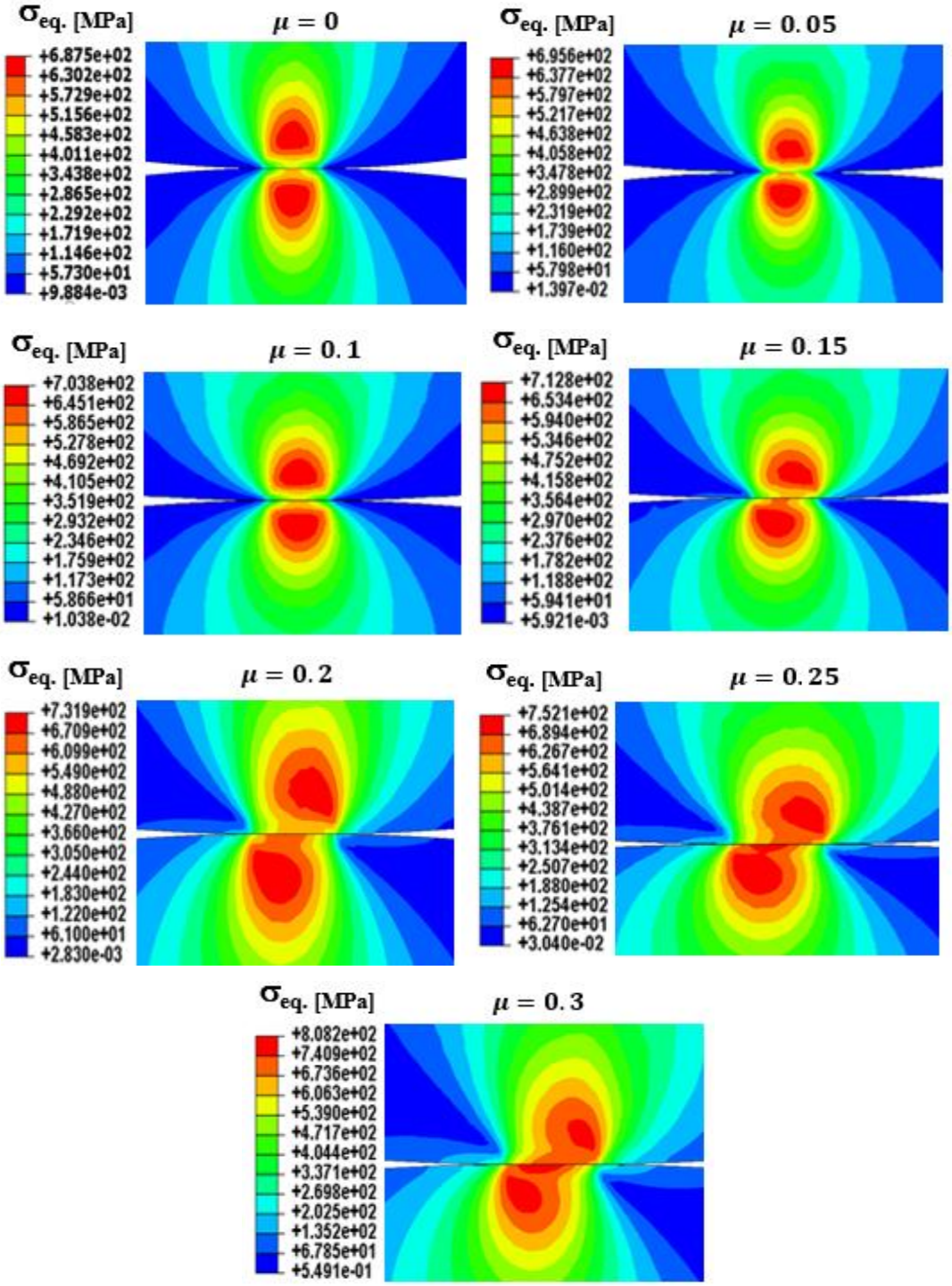

Figure 4. 5 Von Mises stress distribution with different coefficient of friction

As seen from the above figure 4.5 as the friction between the contacts decrease the Von Mises stress profile becomes symmetrical between the contact elements starts from less than μ=0.1 but when the friction increases more than μ=0.1 the stress profile between the contact elements will change or divert out of symmetry.

The results of the simulations for different values of frictional coefficient μ where the resulting distribution of the Von-Mises equivalent stress along the *z*-axis of the contact area (depth under the contact surface) is given. For all given simulations the maximum contact pressure P_0=1210MPa has been considered, which resulted from the normal compressive force F_N=475N

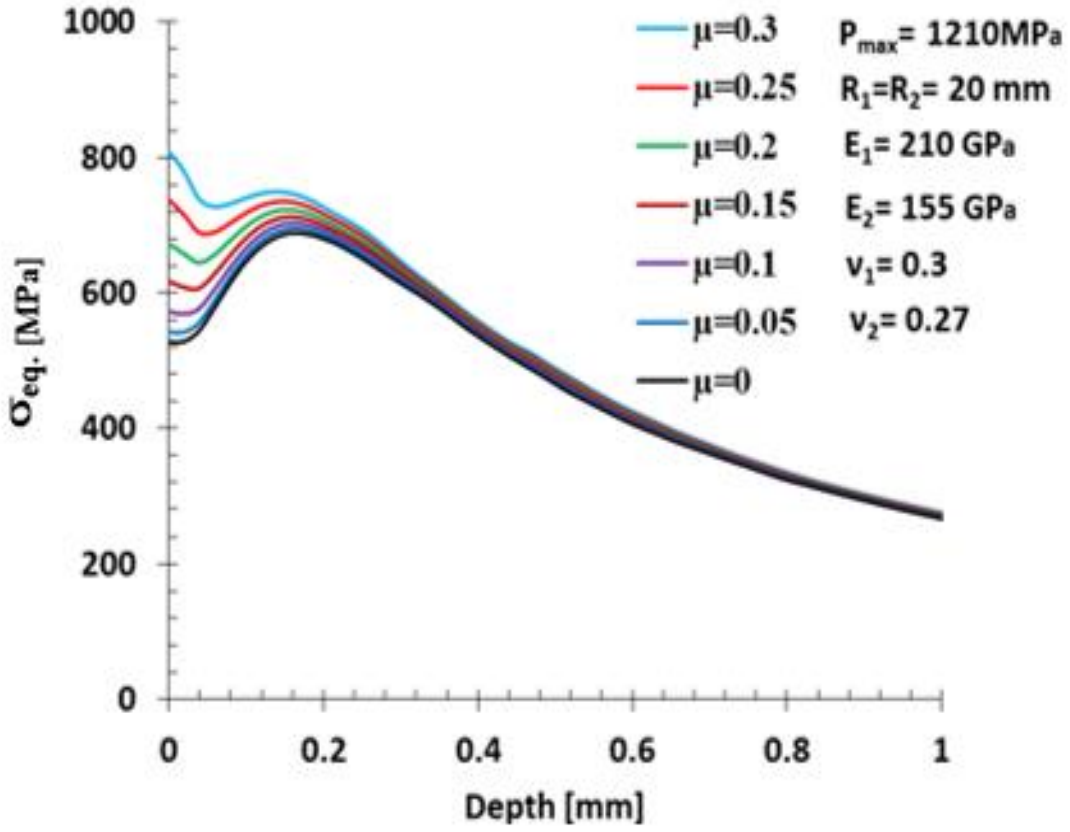

Figure 4. 6 Frictional coefficient effect on mechanical Von Mises stress along depth

From the Simulations shown that for different values of friction μ the influence on the equivalent Von-Mises stress in the depth of contact area. With decreasing the coefficient of friction decrease the equivalent Von-Mises stress and goes far from the surface to the maximum depth of 157µm (Z=0.63b) starting at a friction coefficient $\mu < 0.1$and so with increase the coefficient of friction also increases the maximum equivalent Von-Mises stress reaches to the contact surface while its position under the contact surface depends on both friction and the maximum contact pressure.

And similarly the simulation result verifies that the frictional coefficient has no significant effect on the contact pressure of the contact width and little influence at the starting and ending of contact as shown in the figure 4.7 below.

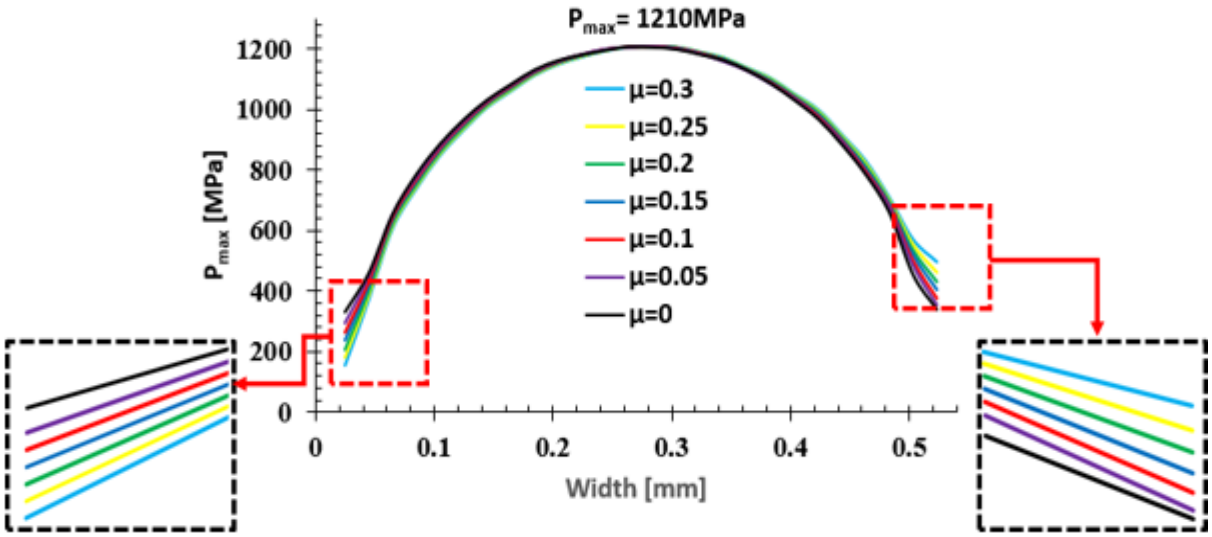

Figure 4. 7 The effect of friction on contact pressure along the contact width

The smallest contact pressure at the starting (inlet) relatively greater for the contact pressure at the ending of contact (exit) at the maximum coefficient of friction and vice versa at the lowest coefficient of friction. Shows that increase the coefficient of friction decreasing the contact pressure at the starting contact and increasing the contact pressure at the ending of contact relative to each other,

4.1.3. Modeling of crack propagation under the effect of friction and lubrication

Crack propagation in a pre-alloyed steel subjected under rolling-sliding contact was studied using finite element method at a maximum applied load (950 MPa). The nucleated surface crack that was observed by the experimental study, the length is 23 μm, was inserted in the model. Then, the effect of friction and pressure on surface crack were analyzed based on:

a) No crack friction and lubricant pressure

b) At variable crack face friction with lubrication but not induced a pressure

c) At variable contact friction

d) Lubricate induces pressure on the crack face.

The Stress intensity factor at the crack tip is determined for the comparison with the fracture toughness of the material at 950MPa and 760MPa contact pressure.

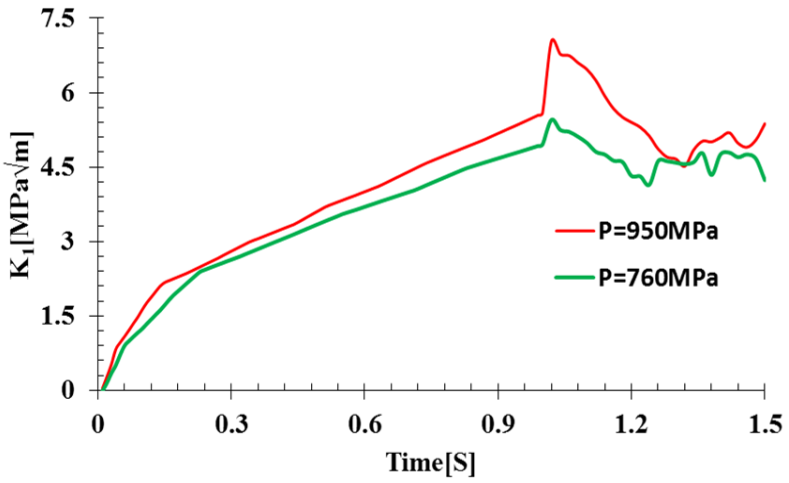

Figure 4. 8 K_I value at different contact pressure

The K_I value increases for some value up to the compressive load applying step and while the mechanical element rotates the stress intensity factor sinusoidal varies at some range

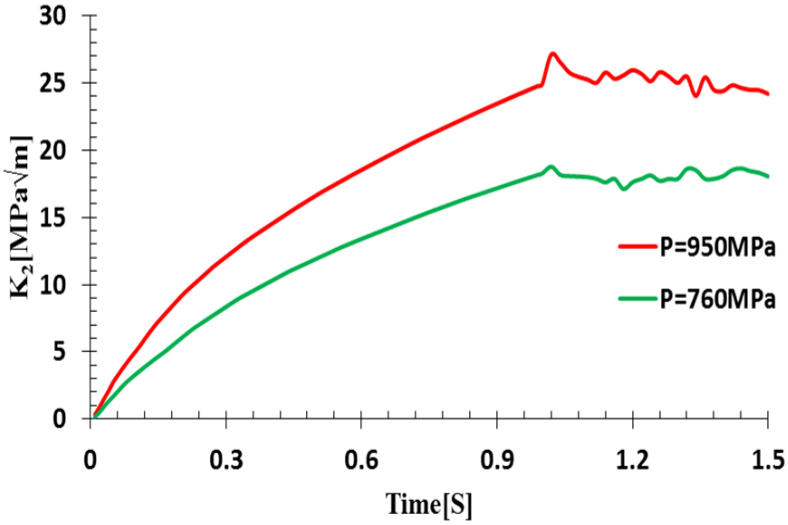

Figure 4. 9 K_{II} value at different contact pressure

The crack propagates in shear mode where the value of K_{II} is greater than K_I around the sharp crack tip in which the stress intensity factor increase to some maximum level.

Table 4. 2 Stress intensity factor value at different contact pressure

	P=950MPa			P=760MPa		
	K_1	K_2	K_{eq}	K_1	K_2	K_{eq}
Numerical	6.77	27.04	28	5.45	18.05	18.85
Fracture toughness			27			27
Crack status			propagated			Not propagated

According to the SIF numerical results, XFEM K_{II} greater than K_I values which shows the crack propagates in mixed mode and at a pressure of 950MPa. The crack propagates where the numerical stress intensity factor greater than material fracture toughness. Thus very good comparison agreement exists between SIFs obtained using XFEM and fracture toughness of the material from the experimental results on the propagation of the crack.

Figure 4.10 represents the crack propagation at different cyclic steps with applying only 950 MPa and 0.3 contact surface frictions.

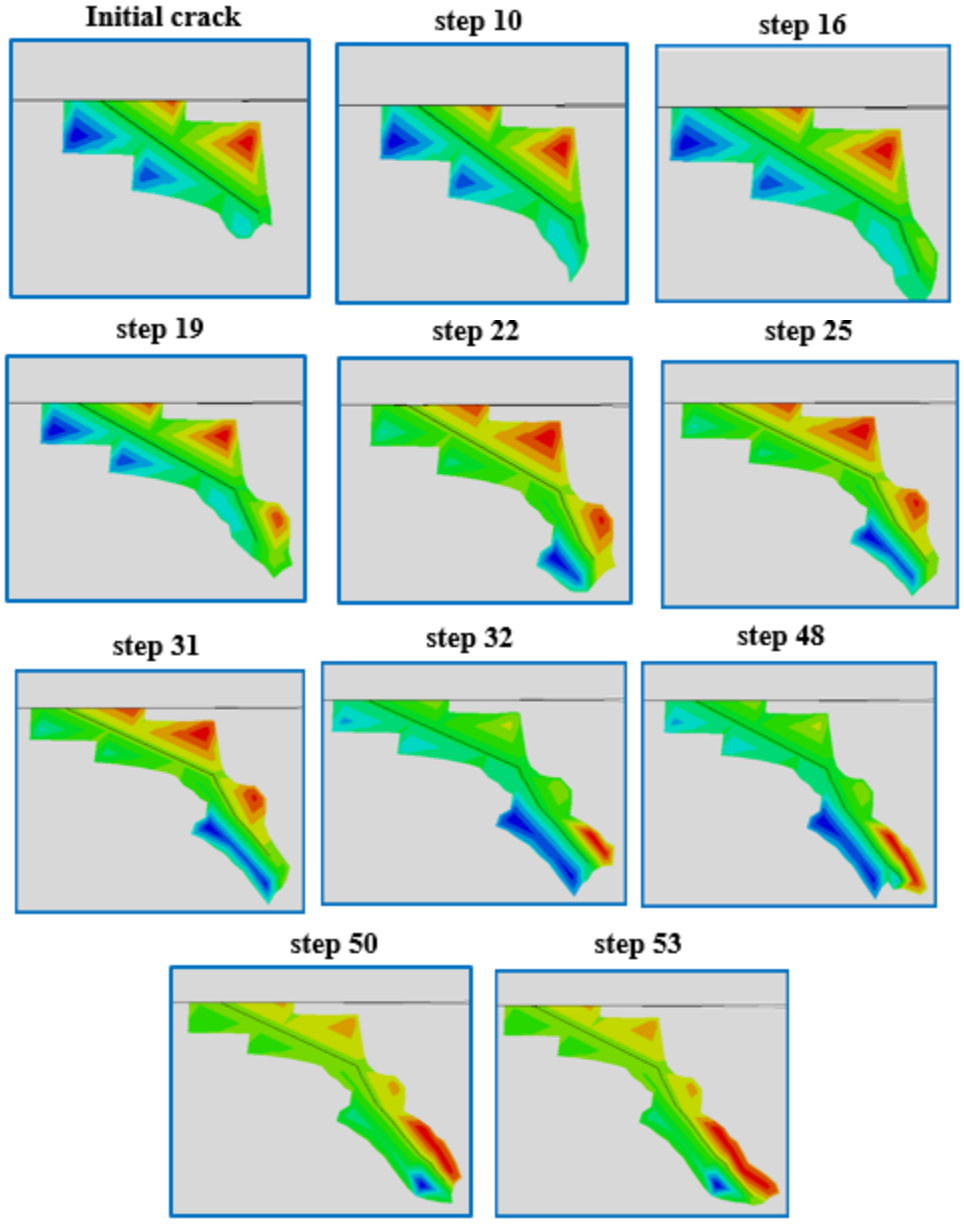

Figure 4. 10 The PHILSM output function of crack propagation with an increasing cyclic load

With the constant force that was applied in the complete contact Abaqus model when the cyclic rotation increase the crack propagates with the step increasing to a maximum crack depth and the relative crack growth becomes larger. The final crack was evaluated at 53 step and it remain constant through the rest simulation step. Figure 4.11 represents the crack propagation at step 53.

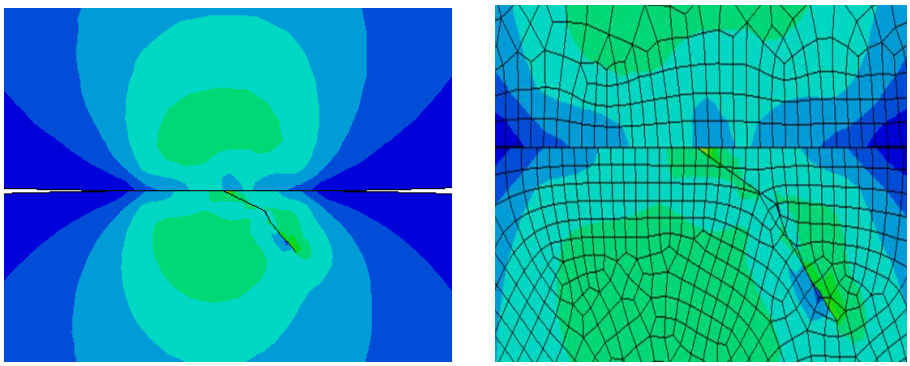

Figure 4. 11 The XFEM output function.

The initial crack is propagated in the direction of maximum energy release rate direction to a maximum depth of 176 µm in a mixed mode behavior.

Figure 4.12 Illustrates the effect of friction between the crack face on crack propagation (lubricant acts only as lubricant).

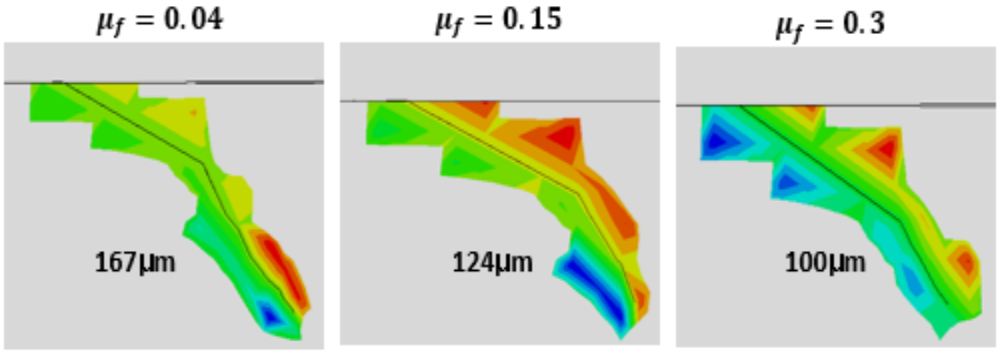

Figure 4. 12 Crack propagation pattern due to the effect of friction between the crack face

The numerical results prove that the depth of crack propagation produced by the roller in the case of dry friction is much less than that of the wet friction. Dry friction has a relatively high coefficient of friction, so it is not easy to produce pitting holes. Result shows that as the friction between the crack face decrease the crack propagation increase or in other words, friction between the faces of crack is the good natural mechanism for suppression of crack propagation. The fluid may lubricate the faces of the crack, without exert a pressure on the crack faces. In this case the fluid could reduce the friction forces acting between the surfaces of the crack, so the crack may be propagating in a shear mode.

Table 4. 3 Parametric influence on crack propagation depth

μ_f	μ	θ	P_{max}	Crack depth	
				initial	final
0.04	0.3	25^0	1210 MPa	10 µm	167µm
0.15	0.3	25^0	1210 MPa	10 µm	124µm
0.3	0.3	25^0	1210 MPa	10 µm	100µm

The table shows that the depth of crack growth angle increases as the friction coefficient decrease, reaching the maximum value of 167um.

And also the effect of contact surface friction on crack propagation is seen with below figure.

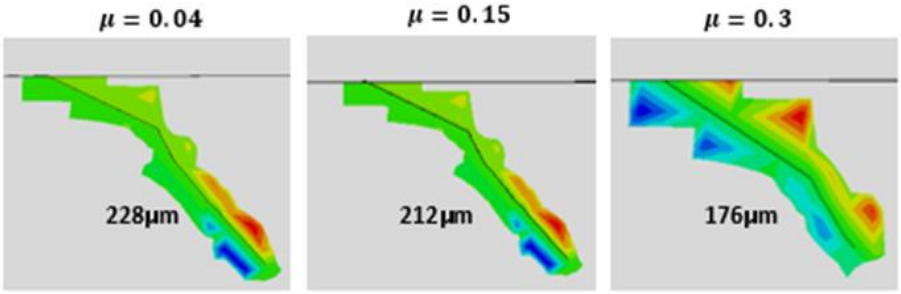

Figure 4. 13 The effect of surface contact friction on crack propagation

As the friction between the contacts rolling sliding mechanical elements decrease the crack increase Since the friction decrease the maximum equivalent Von Mises stress occur at depth from the surface which is responsible for the crack propagation near the maximum equivalent stress.

Table 4. 4 Effect of friction surface on depth of crack propagation

μ	θ	p_{max}	Crack depth	
			Initial	Final
0.04	25^0	1210	10µm	228µm
0.15	25^0	1210	10µm	212µm
0.3	25^0	1210	10µm	176µm

When the lubricant induced a pressure on the crack face its effect for well lubricated with coefficient of friction according to different literature review µ=0.04 is simulated and shows that the depth of crack propagation increases to a maximum of 467µm due to mixed mode increase for a maximum of 165.3% than without considering the effect of lubrication pressure on the crack face

due to wet friction that has relatively low coefficient of friction, with the presence of a grinding fluid, causes the hydraulic surface of the crack face surface to be exposed in facilitating the rate of surface breaking crack propagation. When the pressure on the crack is high the faces of the crack cannot slide relative to each other due to high friction, so that the friction between the crack faces has no influence on the opening.

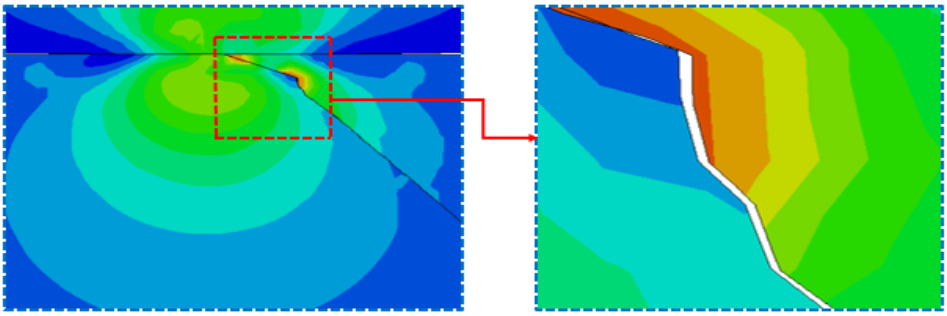

Figure 4. 14 Detail view of crack opening & propagation under the effect of lubricant pressure

Using a deformation scale factor, opened crack is visible and simulations of the result shows fig 4.14 that the lubricant acts as a catalyst inside the crack face by converting the compressive contact load into a crack opening mode, tensile fatigue mechanism, through the effect of fluid pressurization inside the crack face.

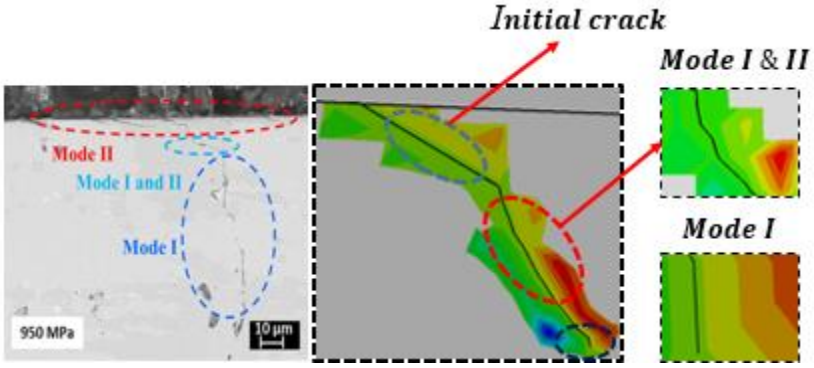

Figure 4. 15 Mode of failure comparison

This result shows that as that of experimental where the crack propagates at 960MPa in mixed mode behavior, shear mode as well as open mode which shows consistency in failure of mode at the given experimental load.

Chapter Five: Conclusions, Recommendations and Future Work

5.1. Conclusions

A numerical analysis is considered to study the surface fracture of a porous carbonized pre-alloyed steel that is tested under rolling sliding contact fatigue load to predict surface crack. The effect of applied load and contact friction on the equivalent stress and pressure distribution is incorporated. In addition crack propagation under the effect of lubricant pressure and friction coefficient is also investigated. An equivalent two-dimensional Hertzian contact model using numerically computational analysis method with XFEM under rolling sliding contact is used.

Numerical XFEM results, shows that the material for a mean pressure of 950MPa cause crack propagated to a length of 176 μm in a mixed mode behavior. When friction between the crack face and the surface to surface contact elements decrease the crack propagation increase and crack growth reaches a maximum of 467μm with effect of lubrication pressure on the crack face.

With decreasing the coefficient of friction decrease the equivalent Von Mises stress and goes far from the surface to the maximum depth of 157μm (Z=0.63b) and increase the coefficient friction reaches maximum equivalent Von-Mises stress to the contact surface.

The frictional coefficient has no significant effect on the contact pressure of the contact width but little influence at the starting and ending of contact. The numerically predicted crack propagation result at the experimental load shows in consistency.

5.2. Recommendations

Crack formation on rolling sliding contact elements is complicated and high cycle process so that sensitive design, regular scheduled maintenance and fast correction monitoring is required for minimizing failure due to crack propagation. Regard on the study results the following recommendations are important for future analysis:

- Use quasi static, simplified equivalent modelling system and convergent simulation time is help full for better convergent analysis solution in determining the contact stress, crack initiation and propagation analysis.
- Use XFEM for crack propagation analysis which has really become a very important generalization of classical finite element technique to decrease the disadvantages of mesh-dependencies of the solutions by establishing mesh-independent.

- Simplified assumptions has been applied to simulate the effect of lubricant/crack interaction inside an RSC crack as it rolls over the contact mechanical elements results for better accuracy.
- Use contact pressure is taken as the same as the pressure created by the lubrication inside the crack face
- Studying of the crack at different load is helpful to know at which critical load does the crack start to grow

5.3. Future Work

During study of this thesis work, there are some research gaps seen while modeling cracks in mechanical rolling sliding contact elements which required Future work. To fill these gaps further deeper analysis investigation is required. Here are these points:

- Further studies require to understanding the influence of the microstructure of the material on the fatigue life, crack initiation and propagation.
- Study should make the influence of the material modelling property variation of carburized surface and the UN-carbonizes surface in the depth direction of the same material on crack initiation and propagation.
- Considering the effect of elastic hydro dynamic and hydrodynamic lubrication (fluid film thickness) on contact stress, contact pressure, crack initiation, crack propagation and fatigue life of contacting elements.
- Effect of lubricant temperature on crack initiation and propagation as well as experimental validation
- Effect of 3D Modelling analysis to see the effect of lubricant pressure on the crack face width

References

[1] J. H. Melson, R. L. West, N. E. Dowling, and J. M. Kennedy, "Fatigue Crack Growth Analysis with Finite Element Methods and a Monte Carlo Simulation," 2014.

[2] M. Ghodrati, M. Ahmadian, and R. Mirzaeifar, "Modeling of Rolling Contact Fatigue in Rails at the Microstructural Level," *Wear*, 2018.

[3] C. Springs, L. Xin, V. L. Markine, and I. Y. Shevtsov, "Numerical Analysis of Rolling Contact Fatigue Crack Initiation and Fatigue Life Prediction of the Railway Crossing."

[4] J. E. Garnham and J. H. Beynon, "The early detection of rolling-sliding contact fatigue cracks," vol. 44, pp. 103–116, 1991.

[5] D. Hannes and B. Alfredsson, "Modelling of surface initiated rolling contact fatigue damage," *Procedia Eng.*, vol. 66, pp. 766–774, 2013.

[6] S. Tesfaye, A. Molinari, and W. Pahl, "Damage phenomena in lubricated rolling- sliding wear of a gas carburised 0 . 85 % Mo low- alloyed sintered steel : theoretical analysis and experimental verification," vol. 5899, November, 2017.

[7] R. L. Jackson, H. Ghaednia, H. Lee, A. Rostami, and X. Wang, *Contact Mechanics*. 2013.

[8] G. Fajdiga, "Computinal fatigue analysis of contacting mechanical elements," vol. 3651, pp. 169–175, 2015.

[9] R. Ismail, Running-in of Rolling-sliding Contacts. 2013.

[10] S. T. Mekonone, W. Pahl, and A. Molinari, "Influence of the microstructure on the subsurface and surface damage during lubricated rolling – sliding wear of sintered steel : theoretical analysis and experimental investigation," vol. 5899, 2018.

[11] V. Hegadekatte, S. Kurzenhäuser, N. Huber, and O. Kraft, "A predictive modeling scheme for wear in tribometers," *Tribol. Int.*, vol. 41, no. 11, pp. 1020–1031, 2008.

[12] K. C. Yadav and M. Verma, "Review of Tribology (Friction , Wear & Lubrication) study on Titanium and its Alloy surfaces," no. February, pp. 58–63, 2016.

[13] G. Discussion, Tribology 9.1, no. 1997. 2014.

[14] S. Affatato and L. Grillini, 1 - Topography in bio-tribocorrosion. Woodhead Publishing Limited, 2013.

[15] F. Öhnander, "An Attempt Towards FE-Modelling of Fracture Propagation in Railway Wheels," 2018.

[16] S. A. Alshahrany, "Rolling contact fatigue in heavily loaded gear transmission contact s

by," November, 2015.

[17] K. J. B. Chari, "Licensed Under Creative Commons Attribution CC BY Investigation on Mode – Investigation on Mode – I Fracture Parameters Using Steel Fibers in High Strength Concrete," December, pp. 1–8, 2016.

[18] Y. Kadin and A. V Rychahivskyy, "Modeling of surface cracks in rolling contact," *Mater. Sci. Eng. A*, vol. 541, pp. 143–151, 2012.

[19] R. Hojjati-Talemi, Numerical Modelling Techniques for Fretting Fatigue Crack Initiation and Propagation. 2014.

[20] B. Ernst and W. Jensen, "Master Thesis Numerical Analysis of Crack Propagation Fracture Mechanics and Numerical Programming," June, 2015.

[21] J. H. Langeland, "Finite Element Analysis of the fatigue strength of a big-end bolt Master Thesis in Energy Technology Thermal Machines Jan Harald Langeland Faculty of Mathematics and Natural Sciences University of Bergen Western Norway University of," June, 2017.

[22] S. Vethe, "Numerical simulation of fatigue crack growth," June, 2012.

[23] R. Balcombe, "A study of rolling contact fatigue cracks in lubricated contacts By," April, 2012.

[24] D. I. Ã. Fletcher, P. Hyde, and A. Kapoor, "Investigating fluid penetration of rolling contact fatigue cracks in rails using a newly developed full-scale test facility," vol. 221, pp. 35–45, 2007.

[25] S. Ancellotti, M. Benedetti, M. Dallago, and V. Fontanari, "Fluid Pressurization and Entrapment Effects on the SIFs of Cracks produced under lubricated Rolling-Sliding Contact Fatigue," Procedia Struct. Integr., vol. 2, pp. 3098–3108, 2016.

[26] A. E. Azianou, K. Debray, F. Bolaers, P. Chiozzi, and F. Palleschi, "Modeling of the Behavior of a Deep Groove Ball Bearing in Its Housing," vol. 2013, October, pp. 45–50, 2013.

[27] V. Nikoli and I. Atanasovska, "The analysis of contact stress on meshed teeth's flanks along the path of contact for a tooth pair," vol. 3, pp. 1055–1066, 2003.

[28] P. S. Rao, N. Sriraj, and M. Farookh, "Contact Stress Analysis of Spur Gear for Different Materials using Anysis and Hertz Equation," vol. 1, no. 1, pp. 45–52, 2015.

[29] I. Atanasovska, "Finite Element Model for Stress Analysis and Nonlinear Contact Analysis

of Helical Gears," no. 1, pp. 61–69, 2009.

[30] P. Taylor, W. Cheng, H. S. Cheng, and L. M. Keer, "Experimental Investigation on Rolling / Sliding Contact Fatigue Crack Initiation with Artificial Defects," January 2015, pp. 37–41, 2008.

[31] L. M. Keer, Q. Wang, and D. Zhu, "Effect of Surface Topography on Contact Fatigue in Mixed Lubrication Effect of Surface Topography on Contact Fatigue in Mixed Lubrication ©," February 2016, 2003.

[32] T. Makino, Y. Neishi, D. Shiozawa, Y. Fukuda, K. Kajiwara, and Y. Nakai, "Evaluation of rolling contact fatigue crack path in high strength steel with artificial defects," *Int. J. Fatigue*, vol. 68, pp. 168–177, 2014.

[33] K. Sharma, I. V Singh, B. K. Mishra, and V. Bhasin, "Numerical Modeling of Part-Through Cracks in Pipe and Pipe Bend using XFEM," Procedia Mater. Sci., vol. 6, no. Icmpc, pp. 72–79, 2014.

[34] A. M. Mode, F. Crack, G. Model, A. To, and C. Fatigue, "WTC2005-63331," pp. 9–10, 2005.

[35] W. Yang, "Modelling recycled aggregate concrete crack by extended finite element method and concrete damage plasticity May 2016."

[36] N. Govindarajan and R. Gnanamoorthy, "Rolling / sliding contact fatigue life prediction of sintered and hardened steels," vol. 262, pp. 70–78, 2007.

[37] C. Santus, M. Beghini, I. Bartilotta, and M. Facchini, "Surface and subsurface rolling contact fatigue characteristic depths and proposal of stress indexes," *Int. J. Fatigue*, vol. 45, pp. 71–81, 2012.

[38] S. Marble, "Numerical Modeling of Mixed Lubrication and Flash Temperature in EHL Elliptical," vol. 130, January, pp. 1–20, 2008.

[39] P. Purushothaman and P. Thankachan, "Hertz Contact Stress Analysis and Validation," vol. 2, Xi, pp. 531–538, 2014.

[40] Z. Golmohammadi, A. Walvekar, and F. Sadeghi, "A 3D efficient finite element model to simulate rolling contact fatigue under high loading conditions," Tribol. Int., 2018.

[41] D. Hannes and B. Alfredsson, "Numerical investigation of the spall opening angle of surface initiated rolling contact fatigue," Eng. Fract. Mech., vol. 131, pp. 538–556, 2014.

[42] W. Pu, D. Zhu, J. Wang, and Q. J. Wang, "Rolling-Sliding Contact Fatigue of Surfaces

with," Int. J. Fatigue, 2016.

[43] J. Jurenka and M. Španiel, "Advances in Engineering Software Advanced FE model for simulation of pitting crack growth," Adv. Eng. Softw., vol. 72, pp. 218–225, 2014.

[44] F. Li, W. Hu, Q. Meng, Z. Zhan, and F. Shen, "A new damage-mechanics-based model for rolling contact fatigue analysis of cylindrical roller bearing," Tribol. Int., 2018.

[45] O. Slávik, P. Hutař, M. Berer, A. Gosch, F. Arbeiter, and G. Pinter, "Numerical Modelling of Cylindrical Specimen under Mixed-Mode Loading Conditions," vol. 774, pp. 325–330, 2018.

[46] M. Bozkurt, A. O. Ayhan, and M. F. Yaren, "Finite element modeling and experimental studies on mixed mode-I/III fracture specimens," vol. 35, pp. 350–359, 2016.

[47] R. Citarella and M. Perrella, "Surface Crack Subject to Mixed Mode Loading : Numerical Simulations and Experimental Tests."

[48] T. He, "Simulation of Plasto- Elastohydrodynamic Lubrication in a Rolling Contact," vol. 138, July 2016, pp. 1–12, 2017.

[49] J. Flas, B. Zafos, and R. Potoc, "Numerical modelling of crack path in the lubricated rolling – sliding contact problems," vol. 75, pp. 880–891, 2008.

[50] C. Klaassen, A. Crawford, A. K. Prathuru, and R. Gordon, "Mixed-mode surface fracture characterstics of metal-to -metal adhesively bonded joints: expermental and simulation method," Procedia Struct. Integr., vol. 5, pp. 40–47, 2017.

[51] R. Vijaywargiya and I. Green, "Author ' s personal copy A finite element study of the deformations , forces , stress formations , and energy losses in sliding cylindrical contacts," vol. 42, pp. 914–927, 2007.

[52] P. Bocher, "Finite Element Analysis Simulation of the Effect of Induction Hardening on Rolling Contact Fatigue," vol. 140, November, pp. 1–10, 2018.

[53] S. Ancellotti, M. Dallago, and V. Fontanari, "Lubricating Fluid Pressurization and Entrapment in Inclined Edge Cracks Under Rolling-Sliding Contact Fatigue," January 2016, 2015.

[54] Y. . B. TEZ, "Effect of height and loading span on the fracture toughness of disc type rock specimens under three point bending," May, 2008.

[55] C. A. E. User, "Dessault systems, Abaqus Manual, 2012."

[56] S. Naga, V. Ravi, and K. Kurapati, "ElasticC-plastic indentation deformation in

homogeneous and layered materials : finite element analysis," 2008.